

STRUCTURAL, VIBRATIONAL AND ELECTRONIC PROPERTIES OF SOME TETREL-BONDED COMPLEXES OF THE FLUORINATED METHANES METHYL FLUORIDE, DIFLUOROMETHANE AND FLUOROFORM. AN AB INITIO STUDY

Thomas Ford¹ and Ponnadurai Ramasami²

¹University of KwaZulu-Natal

²University of Mauritius

March 17, 2022

Abstract

A search has been conducted, employing ab initio molecular orbital theory, for potential tetrel-bonded complexes between the fluorinated methanes methyl fluoride, difluoromethane and fluoroform, and the related hydrides ammonia, water, hydrogen fluoride, phosphine, hydrogen sulfide and hydrogen chloride. Eleven such complexes have been identified, six containing CH₃F and five CH₂F₂. The complexes are typically less strongly bound than their hydrogen-bonded counterparts, and the interaction energies vary in a consistent way with the periodic trend of the electron donors. The intermolecular separations and changes of the relevant intramolecular bond lengths, the wavenumber shifts of the critical vibrational modes, and the extents of charge transfer for the atoms most closely involved in the interactions correlate, by and large, with the strengths of interaction.

STRUCTURAL, VIBRATIONAL AND ELECTRONIC PROPERTIES
OF SOME TETREL-BONDED COMPLEXES OF THE FLUORINATED METHANES
METHYL FLUORIDE, DIFLUOROMETHANE AND FLUOROFORM.
AN *AB INITIO* STUDY

Ponnadurai Ramasami^{a,b} and Thomas A. Ford^{c,*}

^a Computational Chemistry Group, Department of Chemistry, Faculty of Science,
University of Mauritius, Réduit 80837, Mauritius

^b Department of Chemistry, University of South Africa,
Private Bag X6, Florida 1710, South Africa

^c School of Chemistry and Physics, University of KwaZulu-Natal, Westville Campus,
Private Bag X54001, Durban 4000, South Africa

*E-mail address: ford@ukzn.ac.za.

ABSTRACT

A search has been conducted, by means of *ab initio* molecular orbital theory, for potential tetrel-bonded complexes between the fluorinated methanes methyl fluoride, difluoromethane and fluoroform, and the related hydrides ammonia, water, hydrogen fluoride, phosphine, hydrogen sulphide and hydrogen chloride. Eleven such complexes have been identified, six containing CH_3F and five CH_2F_2 . The complexes are typically less strongly bound than their hydrogen-bonded counterparts, and the interaction energies vary in a consistent way with the periodic trend of the electron donors. The intermolecular separations and changes of the relevant intramolecular bond lengths, the wavenumber shifts of the critical vibrational modes, and the extents of charge transfer for the atoms most closely involved in the interactions correlate, by and large, with the strengths of interaction.

Keywords: *ab initio* ; intermolecular complexes; tetrel bonds; structures; vibrational spectra.

1. Introduction The carbon bond interaction [1-4] is one of a family of non-covalent interactions [5] in which a nucleophile donates electronic charge into a $\text{CX } \sigma^*$ orbital at the carbon “end” of the CX bond. This interaction has subsequently been described as a tetrel bond, in order to recognize that such attractions can also occur with other atoms of the tetrel group, group 14, namely Si, Ge, Sn and Pb [6-10]. Non-covalent interactions have generated a great deal of interest in recent years, and the halogen bond [11-14], chalcogen bond [15,16], pnictogen bond [17-19] and triel bond [20-22], associated with electron acceptor atoms of elements of groups 17, 16, 15 and 13, have been the subject of numerous important studies. Including the hydrogen [23], lithium [24] and beryllium bonds [25], this range of non-covalent interactions now covers representative elements of the main groups of the entire periodic table, with the exception of group 18. We have reported our studies of the complexes formed between the fluorinated methanes methyl fluoride, difluoromethane [26] and fluoroform [27], and the hydrides XH_n ($X = \text{N, O, F, P, S, Cl}$, $n = 1$ to 3), in an effort to identify the presence of blue-shifting hydrogen bonds [5,28], which might be responsible for the stabilities of the complexes. This range of substituted methane derivatives suggests that alternative structures may exist for the adducts, in which stability is attributed to the existence of tetrel-bonded interactions. We have therefore undertaken a comprehensive study of the properties of the potential tetrel-bonded complexes formed between the same three substituted methanes and the six hydrides, representing a 3×6 matrix of binary adducts, of which it was hoped that at least some might be found to possess isomeric structures which could be described as being tetrel-bonded. Numerous papers have been devoted to experimental spectroscopic studies of complexes of difluoromethane [29] and fluoroform [30-35] and the electron donors of interest here, particularly in the gas phase and in cryogenic matrices. These experimental reports have been augmented by a large number of theoretical studies focussed on complexes of CH_3F [26,36-47], CH_2F_2 [26,29,36-42,47] and CHF_3 [27,32-40,42,45,47-55] with NH_3 , H_2O , HF , PH_3 , H_2S and HCl . Apart from the six hydrides of interest in this work, there are reports in the literature of the properties of the complexes of CH_3F , CH_2F_2 and CHF_3 with a variety of other electron donors, both experimentally [33,56-70] and theoretically [33,39,40,43,46,53-55,59,62-66,68,70], ranging in size from N_2 , CO , CO_2 and HCN [46,56,62,68] to tropolone [60]. Since the recognition of the tetrel bond, Mani and Arunan have re-examined the complexes of CH_3F with NH_3 , H_2O , HF , PH_3 , H_2S and HCl [1,2,4] in studies aimed at identifying the existence of tetrel-bonded adducts among this set, paralleling the approach we have adopted in the present work.
2. Computational Methodology The calculations were performed using Gaussian-16 [71], at the second order level of Møller-Plesset perturbation theory [72] and with the aug-cc-pVTZ basis sets of Dunning [73,74]. Interaction energies were computed from the energies of the optimized structures of the complexes and of the interacting monomers, and were corrected for basis set superposition error (BSSE) [75] by the counterpoise procedure of Boys and Bernardi [76], and for vibrational zero-point energy differences. The interaction energies were decomposed into their various components (electrostatics, exchange, induction and dispersion) using symmetry-adapted perturbation (SAPT) theory [77], by making use of the Psi4 code of Turney and co-workers [78]. The specific interactions among the various monomer molecular orbitals which were responsible for the stabilities of the complexes were revealed by using Weinhold’s natural bond orbital (NBO) theory [79] through version 3.1 of the NBO program

[80] implemented in the Gaussian-16 suite [71].

3. Results and Discussion
4. Molecular Structures

The properties of the minimum energy structures of the methyl fluoride complexes are set out in Table 1, which describes the structures and lists the point groups and minimized energies of each species. The corresponding results for the hydrogen-bonded complexes reported earlier [26] are included for comparison. The structures are illustrated in Figure 1, which indicates that the interactions responsible are uniformly C...X tetrel-bonded, in which a lone pair orbital on the X atom of the nucleophile approaches the CH₃F tetrahedron perpendicularly to the HHH face and interacts with the $\sigma^*(\text{CF})$ orbital. These findings are consistent with those of Mani and Arunan [1,2,4].

In the case of the CH₂F₂ complexes, two possibilities present themselves, one in which the electron donor approaches the CH₂F₂ tetrahedron via a HHH face, interacting through a $\sigma^*(\text{CF})$ orbital (structure 1) and the other in which it presents through a HFF face, interacting with a $\sigma^*(\text{CH})$ orbital (structure 2). This distinction has also been observed by Scheiner *et al.* [36,39,40,42]. The results for the structure 1 complexes are shown in Table 2 and indicate that in all cases except that of the CH₂F₂.HF complex, interaction is through a C...X tetrel bond. Table 2 also includes the corresponding results for the hydrogen-bonded series [26]. The exception among the structure 1 adducts is that of the CH₂F₂.HF complex, which relaxed to a FH...F hydrogen-bonded isomer. These structures are shown in Figure 2, which indicates that, based on the apparent close approach of some of the atoms, in some cases there is the possibility that a secondary interaction exists, of the XH...F, F...P or F...Cl type (X = N, O, S).

The results for the second possibility (structure 2) are given in Table 3, along with the hydrogen-bonded data [26], and are illustrated in Figure 3. For this series the only complex which exhibits tetrel-bonded behaviour is the CH₂F₂.HCl species, which is stabilized by a C...Cl interaction. This structure is very similar to that of the structure 1 variant (see Table 2 and Figure 2). The five remaining structure 2 complexes feature either CH...N or XH...F hydrogen bonds (X = O, F, P, S).

The complexes featuring CHF₃ are found to be exclusively “reverse hydrogen-bonded” through XH...F (X = N, F, P, S, Cl) bonds (see Table 4 and Figure 4), the exception being CHF₃.H₂O, which optimized with the same structure as that found in ref. 27.

Interaction Energies Table 5 lists the interaction energies, corrected for BSSE and for zero-point energy differences, of all 24 complexes, both tetrel-bonded and hydrogen-bonded [26,27]. Among the CH₃F complexes the interaction energies of the tetrel-bonded species are extremely small, and vary over only a small range. They are regularly lower than those of the hydrogen-bonded variants, in some cases substantially so. The computed interaction energies vary almost monotonically in the order NH₃ > H₂O > HF > PH₃ > H₂S > HCl, and they track with the natures of the electron donors in a regular way, correlating with some relevant properties of the donors such as their gas phase basicities [81] and polarizabilities [82]. A plot of the interaction energies *versus* the gas phase basicities is shown in Figure 5a, while the corresponding plot *versus* the polarizabilities is illustrated in Figure 5b. While for the hydrogen-bonded isomers the interaction energies decrease smoothly with increasing gas phase basicity and polarizability of the partner molecule [26], with separate trend lines for the first row and second row electron donors, in the case of the tetrel-bonded variants, the trends are in the reverse direction, although in the tetrel-bonded series the spread of energies is only a little over 3 kJ mol⁻¹. This behaviour indicates a fundamental difference in the natures of hydrogen and tetrel bonding. The interaction energies of the CH₂F₂ complexes (structure 1) are more difficult to interpret, since the structures of the adducts with NH₃, H₂O, PH₃, H₂S and HCl feature the possibility of a second interaction, which would enhance their binding energies. This is particularly evident in the case of the PH₃ and H₂S complexes, where their negative interaction energies are transposed relative to the positions of the donor atoms in the periodic table. The energies separate into two distinct groups, with the NH₃ and H₂O-containing species forming one set and those with PH₃, H₂S and HCl the other, with energies NH₃ [?] H₂O > PH₃ [?] H_[?]S [?] HCl. The plots of the interaction energies *versus* the gas phase basicities (Figure 6a) and polarizabilities (Figure 6b) confirm the inverse dependences on these properties

for the hydrogen-bonded species [26] and the tetrel-bonded analogues, apart from the anomalous data point for the HCl adduct. The structure 2 variant of the $\text{CH}_2\text{F}_2\cdot\text{HCl}$ complex is the only one of this set which shows tetrel-bonded behaviour, and has very similar properties to those of the structure 1 counterpart. All six of the complexes with CHF_3 are described as “reverse hydrogen-bonded”; five of them involve bonds of the $\text{XH}\dots\text{F}$ type. The exception is the $\text{CHF}_3\cdot\text{H}_2\text{O}$ adduct, which is stabilized by a $\text{CH}\dots\text{O}$ interaction, with a substantially larger binding energy, similar to that found earlier [27]. The remaining five interaction energies depend almost linearly on the gas phase basicities. A SAPT decomposition analysis [77] of the interaction energies into their attractive (electrostatics, induction and dispersion) and repulsive (Pauli exchange) components, for both the tetrel-bonded and hydrogen-bonded families produced the results shown in Tables 6 and 7 respectively. These findings indicate that for the tetrel-bonded adducts the electrostatics contribution dominates the dispersion for the first row donors, but that the reverse is true for the second row analogues; in either case the electrostatics and dispersion components decrease fairly regularly in parallel with the total interaction energies. The induction component is a minor contributor to the binding process. For the hydrogen-bonded series, on the other hand, the electrostatics contributions, and to a lesser extent the dispersion terms, increase steadily with increasing total interaction energy, while the induction component makes a far more significant contribution. A further distinction between the tetrel-bonded and hydrogen-bonded series is that in the first case the exchange contribution decreases regularly in the orders $\text{NH}_3 > \text{H}_2\text{O} > \text{HF}$ and $\text{PH}_3 > \text{H}_2\text{S} > \text{HCl}$, while for the second group the exchange term varies consistently in the reverse direction. These distinctions between the relative importances of the various components of the interaction energy help to explain the fundamental differences in the ways in which the hydrogen-bonded and tetrel-bonded complexes achieve their stability. The SAPT energy decompositions for the CH_2F_2 complexes (Tables 6 and 7) confirm the lack of regularity in the behaviour of the tetrel-bonded set, except that the induction component is relatively unimportant, while the dispersion term is fairly constant. The hydrogen-bonded group shows fairly well-behaved trends in the values of the electrostatics and induction terms, while the dispersion contributions are relatively independent of the nature of the electron donor. The total interaction energies determined at the SAPT2 level (Tables 6 and 7) correlate virtually linearly with those computed using MP2 (see Table 5).

Intermolecular Structural Parameters

The relevant intermolecular geometries of the tetrel-bonded CH_3F complexes are collected in Table S1 of the Supplementary Information. These are the $\text{C}\dots\text{X}$ bond lengths, and the $\text{HC}\dots\text{X}$ and $\text{HX}\dots\text{C}$ bond angles. The $\text{C}\dots\text{X}$ separations correlate directly with the interaction energies, consistent with the dependence of the interaction energies on the gas phase basicities and polarizabilities (Figures 5 and 6). While, for conventional hydrogen-bonded interactions, the separation of the bonded atoms normally decreases with increasing binding energy, the reverse is true for the tetrel-bonded complexes considered here, emphasizing the contrast between the two types of interaction. The $\text{C}\dots\text{X}$ separations are plotted against the interaction energies in Figure 7.

The computed $\text{HC}\dots\text{X}$ angles (Table S1) are remarkably invariant to the nature of the bonding partner, and approximate the complement of the tetrahedral FCH angle, confirming the near linearity of the $\text{FC}\dots\text{X}$ interaction, while the $\text{HX}\dots\text{C}$ angles are determined largely by the values of the internal HCH angles.

The corresponding intermolecular geometry information for the structure 1 series of CH_2F_2 complexes is presented in Table S2 in the Supplementary Information. In addition to the $\text{C}\dots\text{X}$ separations, for the complexes with NH_3 , H_2O , PH_3 , H_2S and HCl there is evidence of a second interaction (see Figure 2). The dependence of the $\text{C}\dots\text{X}$ bond distances on the interaction energies is illustrated in Figure 7, and for the second row donors a similar relationship is observed to that for the CH_3F family of complexes, except for the juxtaposition of the PH_3 and H_2S data. This anomalous situation extends also to the NH_3 and H_2O adducts. The hydrogen-bonded $\text{H}\dots\text{F}$ distances in the complexes with NH_3 , H_2O and H_2S decrease with increasing interaction energies in the expected manner for this type of interaction.

As a consequence of the variety of structural motifs adopted by the CH_2F_2 adducts, the $\text{FC}\dots\text{X}$ angles do not appear to subscribe to a regular pattern (see Table S2), other than that the angles are close to the complements of the FCF angles of the monomers. Similarly the $\text{XH}\dots\text{F}$ and $\text{CF}\dots\text{H}$ angles form two groups

with values close to 120° and 90° respectively, the exception being the PH_3 complex, where the $\text{CP}\dots\text{H}$ angle lying in the symmetry plane is close to 180° .

Changes of Intramolecular Structural Parameters

The perturbations of the intramolecular CF and CH bond lengths of the tetrel-bonded CH_3F complexes are presented in Table S3. The CF changes increase regularly with increasing interaction energy, as shown in Figure 8, in contrast with the expectation for conventional hydrogen-bonded interactions, once again emphasizing the fundamental differences in the natures of the two types of interaction. The changes of the CH bond lengths are minimal. In the case of the CH_2F_2 set of complexes (Table S4), the CF1 bonds are remote from the sites of interaction and are relatively little affected, but the CF4 bonds, which are involved in the secondary interaction in five of the complexes, follow the same pattern as the non-bonded CF bonds of the CH_3F set, and in fact, apart from the $\text{CH}_2\text{F}_2\cdot\text{NH}_3$ outlier, the same virtually linear trend line in Figure 8 fits both families of adducts.

Vibrational Spectroscopic Changes of the CH_3F and CH_2F_2 Molecules Vibrational wavenumber shifts are often the experimentally-determined quantities most sensitive to the strength of intermolecular bonding. The computed wavenumber shifts of the CH_3F vibrations of the tetrel-bonded complexes of CH_3F are listed in Table S5. The modes most affected by the interactions are the CF stretching and the symmetric CH_3 bending modes (both of a_1 symmetry in the isolated monomer). Both modes undergo consistent red shifts, which increase regularly in the orders $\text{HF} < \text{H}_2\text{O} < \text{NH}_3$ and $\text{HCl} < \text{H}_2\text{S} [?] \text{PH}_3$. The dependences of these red shifts on the interaction energies are shown in Figure 9, revealing the expected monotonic relationship, at least for the first row donors. For the second row donors the H_2S data appear rather elevated, compared with those for the PH_3 and HCl complexes. The remaining mode wavenumber shifts of the CH_3F complexes are more modest. For the CH_2F_2 complexes the results are presented in Table S6. The vibrations of interest here are the symmetric (a_1) and antisymmetric (b_2) CH_2 stretching and the CH_2 bending (a_1) modes. In contrast with the CH_3F complex data, while the CH_2 bending mode shifts consistently to the red, the two CH_2 stretching vibrations undergo regular blue shifts. The shifts vary with the interaction energies in the now-familiar way, including the transposition of the PH_3 and H_2S points, as illustrated in Figure 10, the data points for the NH_3 and H_2O complexes also apparently representing anomalies. The variations of the infrared intensities of the vibrations of complexed molecules can sometimes provide useful corroborative spectroscopic information to that presented by the wavenumber shifts, particularly for strongly-bound complexes. The complex/monomer intensity ratios of the vibrations of the CH_3F and CH_2F_2 tetrel-bonded complexes are reported in Tables S7 and S8. Consistent with the weak nature of the tetrel-bonded interactions in the present case, the intensity ratios, with very few exceptions, lie in a band of a factor of two, and consequently provide little additional insight into the nature of the tetrel-bonding phenomenon.

Molecular Orbital Interactions

The identities of the specific molecular orbitals of the interacting monomers whose interactions are responsible for the formation of the complexes are revealed by a natural bond orbital (NBO) analysis [79]. Application of the NBO feature of the Gaussian-16 program [71] yielded the results presented in Tables 8 (CH_3F complexes) and 9 (CH_2F_2 complexes). The corresponding results for the hydrogen-bonded analogues from ref. 26 are shown alongside those for the tetrel-bonded species which constitute the major thrust of this work. In the case of the CH_3F family, the interactions are consistently of the $n - \sigma^*$ nature, with only a single donation; there is no evidence of any back donation in any of the complexes. Where there is more than one lone pair orbital associated with the donor atoms O and F, it is the one with a higher s:p ratio which is favoured for interaction, e.g. $\text{lp}2(\text{O})$ has a ratio of 1.11 while that for $\text{lp}1(\text{F}3)$ is 3.67; the less likely donor orbitals tend to be almost pure p orbitals. For the complexes with H_2S and HCl , by contrast, $\text{lp}2(\text{S})$ and $\text{lp}3(\text{Cl})$ are essentially pure p orbitals, whose axes are almost collinear with the extensions of the CF bonds (see Figure 1). The second order perturbation energies track fairly regularly with the total interaction energies (Table 5), the exception once again being the $\text{CH}_3\text{F}\cdot\text{H}_2\text{S}$ adduct.

Among the hydrogen-bonded series of complexes the major sources of donation are from the fluorine lone

pairs of CH_3F to the $\sigma^*(\text{XH})$ orbitals of the partner molecules. In each case two fluorine lone pairs are involved and it is invariably the lone pair with almost total p character ($1p_3$) which is favoured over $1p_1$, which has a s:p ratio varying from 2.53 to 2.63 (NH_3 , H_2O , PH_3 and H_2S) to 1.95 (HF) and 2.14 (HCl). The orientation of the favoured p orbital axes is close to perpendicular to the direction of the CF bond. The second order perturbation energies for the hydrogen-bonded set are substantially greater than for similar interactions in the tetrel-bonded series – in the case of the HF and HCl complexes by a very large amount. There is evidence in the examples of the NH_3 , HF , PH_3 and H_2S complexes of back donation from N, P and S lone pairs and the $\sigma(\text{F3H7})$ orbital of HF to the $\sigma^*(\text{CH})$ and $\sigma^*(\text{CF})$ orbitals of CH_3F , but these are extremely weak interactions.

As shown in Table 9, the tetrel-bonded complexes of CH_2F_2 are characterized by donation from N, O, P, S and Cl lone pairs of the partner molecule to the $\sigma^*(\text{CF1})$ orbitals of CH_2F_2 , along the extension of the CF1 bond direction, similar to the situation for the corresponding CH_3F adducts; these interactions are very weak. In addition, there is back donation from the F4 atom lone pairs of CH_2F_2 into the $\sigma^*(\text{XH})$ orbitals of the partner molecules, but these secondary interactions are also relatively weak. Figure 2 suggested that there were potential additional interactions between the H atoms of NH_3 , H_2O and H_2S , and the P and Cl atoms of PH_3 and HCl , and the F4 atom of CH_2F_2 , and this is now confirmed by the results of Table 9. Again, donation occurs preferentially from the $1p_3$ lone pair of fluorine atom F4, which is aligned almost perpendicular to the CF4 bond. Among the hydrogen-bonded CH_2F_2 complexes, Table 9 shows that donation occurs from the N, O, P and S lone pairs to the $\sigma^*(\text{CH})$ and $\sigma^*(\text{CF})$ orbitals of CH_2F_2 and there is back donation, mainly from fluorine lone pairs to the $\sigma^*(\text{XH})$ orbitals, but there is also a weak interaction between the $\sigma(\text{CH3})$ and the $\sigma^*(\text{NH7})$ orbitals in $\text{CH}_2\text{F}_2\cdot\text{NH}_3$. The predominant fluorine donor orbital is almost exclusively the $1p_2$, which is essentially pure p. It is noteworthy that by far the strongest hydrogen-bonded interactions among this set are the $\text{FH}\dots\text{F}$ and $\text{ClH}\dots\text{F}$ bonds, with almost linear $\text{XH}\dots\text{F}$ arrangements.

A further important quantity which is relevant to the rationalization of the nature of tetrel-bonded and hydrogen-bonded interactions is the extent of charge transfer experienced by each atom in the complex. This information is also provided by the application of the NBO analysis. The changes in the natural atomic charges for the tetrel-bonded and hydrogen-bonded complexes of CH_3F are given in Table 10. This table also includes the corresponding results for the hydrogen-bonded complexes taken from ref. 26. For the CH_3F family of complexes, understandably the atoms most affected are C and F, the F atom accumulating charge at the expense of the C atom, while the hydrogen atoms are very little affected. The extents of atomic charge transfer for the tetrel-bonded set correlate almost monotonically with the interaction energies, as shown in Figure 11a. The corresponding plot for the hydrogen-bonded analogues is given in Figure 11b, which shows that for the first row donor molecules monotonic correlations exist, but for the second row donors similar, but less convincing, relationships are observed.

Table 11 records the charge shifts for the atoms of the CH_2F_2 complexes; again the most important atoms are C and F4. For the tetrel-bonded series no sensible correlations are observed with either the interaction energy or the position of the donor atom in the periodic table, while among the hydrogen-bonded species the charge shifts become more negative in the order $\text{NH}_3 > \text{H}_2\text{O} > \text{HF}$, but no such trend is apparent for the $\text{PH}_3 - \text{H}_2\text{S} - \text{HCl}$ adducts.

Conclusions Both methyl fluoride and difluoromethane form tetrel-bonded complexes with the set of six hydride electron donors considered here. In the case of the CH_3F complexes, interaction is *via* a lone pair of electrons of the donor atom and the $\sigma^*(\text{CF})$ orbital of CH_3F . For the CH_2F_2 complexes, in addition to the X - C interaction (X = N, O, P, S, Cl) there is a secondary, hydrogen bond, association of the $\text{NH}\dots\text{F}$, $\text{OH}\dots\text{F}$, $\text{FH}\dots\text{F}$ and $\text{SH}\dots\text{F}$ type, or of the $\text{F}\dots\text{P}$ and $\text{F}\dots\text{Cl}$ type. Only for $\text{CH}_2\text{F}_2\cdot\text{HF}$ is this second interaction absent, as a result of the strong, highly directional $\text{FH}\dots\text{F}$ bond, which ensures that the HF fluorine atom is sufficiently remote from the C atom for no $\text{C}\dots\text{F}$ attraction to exist. For any given pair of interacting molecules, the CH_2F_2 complex is consistently more strongly bound than its CH_3F counterpart, due to the additive nature of the two modes of association. The interaction energies of the CH_3F series

of complexes vary in a regular way with the identity of the donor atom, whereas for the CH₂F₂ group the variety of structural motifs precludes any discernible dependence on the position of the donor atom in the periodic table. For both families of adducts, the tetrel-bonded isomer is significantly more weakly bound than its hydrogen-bonded counterpart [26]. The intermolecular C...X distances (X = N, O, F, P, S, Cl) of the CH₃F complexes vary in a regular, predictable way with the computed binding energies, and with some minor exceptions the same is also true of the CH₂F₂ adducts. In addition to the regularity of the intermolecular geometrical features, the changes of the intramolecular CF bond lengths also subscribe to a dependence on the interaction energies, and this dependence extends to a common relationship covering both the CH₃F and the CH₂F₂ sets. The spectroscopic data, characterized by the wavenumber shifts of selected vibrational modes of the electron acceptor molecules, also support the regular variation of the complex properties with the strengths of interaction. Specifically, for the CH₃F complexes, the CF stretching and the symmetric CH₃bending mode shifts, being most intimately connected with the sites of interaction, demonstrate a sensible dependence on the binding energies, and the same observation holds broadly for the perturbations of the symmetric and antisymmetric CH₂ stretching and the CH₂ bending vibrations of the CH₂F₂ adducts. The molecular orbital interactions involved in the formation of the tetrel-bonded complexes indicate that a single X - C electron donation is responsible for the stability of the CH₃F adducts, where X = N, O, F, P, S and Cl. In the case of the CH₂F₂ set a second, usually hydrogen-bonded, but also of the F - P and F - Cl type interaction is present, which augments the tetrel-bonded association. Resulting from the transfer of charge from the hydride molecule to the CH₃F or CH₂F₂ entity, the charges on the C and F atoms redistribute themselves such that in the CH₃F case the terminal F atom accumulates charge at the expense of the C acceptor atom. This is in contrast to the situation for the hydrogen-bonded complex isomers, where both C and F atoms experience increases in their net charges. The pattern is fairly similar in the CH₂F₂ family of complexes, but the charge shifts are smaller and, because of the range of structural motifs in these five adducts, more variable. We conclude that both methyl fluoride and difluoromethane are capable of forming tetrel-bonded complexes with NH₃, H₂O, HF, PH₃, H₂S and HCl, but the resulting adducts are clearly more weakly bound than their hydrogen-bonded isomers. Acknowledgements

This work is based on research supported in part by the National Research Foundation of South Africa (NRF) under Grant Number 2053648. The grantholder acknowledges that any opinions, findings and conclusions or recommendations expressed in any publication generated by NRF-supported research are those of the authors and that the NRF accepts no liability in this regard. The authors also acknowledge the University of KwaZulu-Natal for financial assistance and the Centre for High Performance Computing (South Africa) for the use of computational resources, in particular Dr Anton Lopic for invaluable technical assistance.

References

1. Arunan, E. (2013) *Curr. Sci.*, **105** , 892-894.
2. Mani, D. and Arunan, E. (2013) *Phys. Chem. Chem. Phys.*, **15** , 14377-14383.
3. Mani, D. and Arunan, E. (2014) *J. Phys. Chem. A*, **118** , 10081-10089.
4. Mani, D. and Arunan, E. (2015) in Scheiner, S. (ed.), *Noncovalent Forces, Challenges and Advances in Computational Chemistry and Physics 19*, Springer International Publishing Switzerland, pp. 323-356.
5. Hobza, P. and Müller-Dethlefs, K. (2010) *Non-Covalent Interactions: Theory and Experiment*, RSC Publishing, Cambridge, U.K. 225 pp.
6. Bauza, A., Mooibroek, T.J. and Frontera, A. (2013) *Angew. Chem. Int. Ed.*, **52** , 12317- 12321.
7. Grabowski, S.J. (2014) *Phys. Chem. Chem. Phys.*, **16** , 1824-1834.
8. Marin-Luna, M., Alkorta, I. and Elguero, J. (2017) *Theoret. Chem. Acc.*, **136** :41.
9. Ibrahim, M.A.A., Moussa, N.A.M. and Safy, M.E.A. (2018) *J. Mol. Model.*, **24** :219.
10. Grabowski, S.J. (2018) *Molecules*, **23** :1183.
11. Dumas, J.-M., Peurichard, H. and Gomel, M.J. (1978) *J. Chem. Res., Synopses*, 54-57.
12. Legon, A.C. (2010) *Phys. Chem. Chem. Phys.*, **12** , 7736-7747.
13. Politzer, P. and Murray, J.S. (2013) *ChemPhysChem*, **14** , 278-294.
14. Cavallo, G., Metrangolo, P., Milani, R., Pilati, T., Priimagi, A., Resnati, G. and Terraneo, G. (2016) *Chem. Rev.*, **116** , 2478-2601.

15. Wang, W., Ji, B. and Zhang, Y. (2009) *J. Phys. Chem. A*, **113** , 8132-8135.
16. Oliveira, V., Cremer, D. and Kraka, E. (2017) *J. Phys. Chem. A*, **121** , 6845-6862.
17. Zahn, S., Frank, R. Hey-Hawkins, E. and Kirchner, B. (2011) *Chem. Eur. J.*, **17** , 6034- 6038.
18. Scheiner, S. (2013) *Accounts Chem. Res.*, **46** , 280-288
19. Del Bene, J.E., Alkorta, I. and Elguero, J. (2015) in *Noncovalent Forces – Challenges and Advances in Computational Chemistry and Physics 19*, Scheiner, S. (ed.), Springer International Publishing, Switzerland, pp. 191-263.
20. Grabowski, S.J. (2015) *Molecules*, **20** , 11297-11316.
21. Bauza, A. and Frontera, A. (2017) *Theoret. Chem. Accounts*, **136** :37.
22. Esrafil, M.D. and Mousvian, P. (2018) *Mol. Phys.*, **116** , 388-398.
23. Latimer, W.M. and Rodebush, W.H. (1920) *J. Am. Chem. Soc.*, **42** , 1419-1423.
24. Shigorin, D.N. (1959) *Spectrochim. Acta*, **14** , 198-212.
25. Yanez, M., Sanz, P., Mo, O., Alkorta, I. and Elguero, J. (2009) *J. Chem. Theory Comput.*, **5** , 2763-2771.
26. Ramasami, P. and Ford, T.A. (2018) *Mol. Phys.*, **116** , 1722-1736.
27. Ramasami, P. and Ford, T.A. (2012) *J. Mol. Structure*, **1023** , 163-169.
28. Hobza, P. and Havlas, Z. (2000) *Chem. Rev.*, **100** , 4253-4264.
29. Caminati, W., Melandri, S., Rossi, I. and Favero, P. G. (1999) *J. Am. Chem. Soc.*, **121** , 10098-10101.
30. Paulson, S.L. and Barnes, A.J. (1982) *J. Mol. Structure*, **80** , 151-158.
31. Fraser, G.T., Lovas, F.J., Suenram, R.D. and Nelson, D.D. (1986) *J. Chem. Phys.*, **84** , 5983-5988..
32. Rutkowski, K.S., Herrebout, W.A., Melikova, S.M., Rodziewicz, P., van der Veken, B.J. and Koll, A. (2005) *Spectrochim. Acta A*, **61** , 1595-1602.
33. Herrebout, W.A., Melikova, S.M., Delanoye, S.N., Rutkowski, K.S., Shchepkin, D.N. and van der Veken, B.J. (2005) *J. Phys. Chem. A*, **109** , 3038-3044.
34. Gopi, R., Ramanathan, N. and Sundararajan, K. (2014) *J. Phys. Chem. A*, **118** , 5529- 5539.
35. Gopi, R., Ramanathan, N. and Sundararajan, K. (2016) *Chem. Phys.*, **476** , 36-45.
36. Gu, Y., Kar, T. and Scheiner, S. (2000) *J. Mol. Structure*, **552** , 17-31.
37. Wetmore, S.D., Schofield, R., Smith, D.M. and Radom, L. (2001) *J. Phys. Chem. A*, **195** , 8718-8726.
38. Alkorta, I. and Maluendes, S. (1995) *J. Phys. Chem.*, **99** , 6457-6460.
39. Gu, Y., Kar, T. and Scheiner, S. (1999) *J. Am. Chem. Soc.*, **121** , 9411-9422.
40. Scheiner, S., Gu, Y. and Kar, T. (2000) *J. Mol. Structure (Theochem)*, **500** , 441-452.
41. Monat, J.E., Toczyłowski, R.R. and Cybulski, S.M. (2001) *J. Phys. Chem. A*, **105** , 9004-9013.
42. Scheiner, S. and Kar, T. (2002) *J. Phys. Chem. A*, **106** , 1784-1789.
43. Hyla-Kryspin, I., Haufe, G. and Grimme, S. (2008) *Chem. Phys.*, **346** , 224-236.
44. Rosenberg, R.E. (2012) *J. Phys. Chem. A*, **116** , 10842-10849.
45. Hobza, P., Mulder, F. and Sandorfy, C. (1981) *J. Am. Chem. Soc.*, **103** , 1360-1366.
46. Buckingham, A.D. and Fowler, P.W. (1985) *Can. J. Chem.*, **63** , 2018-2025.
47. Kryachko, E.S. and Zeegers-Huyskens, T. (2001) *J. Phys. Chem. A*, **105** , 7118-7125.
48. Zierkiewicz, W., Michalska, D., Havlas, Z. and Hobza, P. (2002) *ChemPhysChem*, **3** , 511-518.
49. Li, X., Liu, L. and Schlegel, H.B. (2002) *J. Am. Chem. Soc.*, **124** , 9639-9647.
50. Alabugin, I.V., Manoharan, M., Peabody, S. and Weinhold, F. (2003) *J. Am. Chem. Soc.*, **125** , 5973-5987.
51. Pejov, L. and Hermansson, K. (2003) *J. Chem. Phys.*, **119** , 313-324.
52. Rhee, S.K., Kim, S.H., Lee, S. and Lee, J.Y. (2004) *Chem. Phys.*, **297** , 21-29.
53. Rodziewicz, P., Rutkowski, K.S., Melikova, S.M. and Koll, A. (2005) *ChemPhysChem*, **6** , 1282-1292.
54. Martins, J.B.L., Politi, J.R.S., Garcia, E., Vilela, A.F.A. and Gargano, R. (2009) *J. Phys. Chem. A*, **113** , 14818-14823.
55. Man, N.T.H., Nhan, P.L., Vo, V., Quang, D.T. and Trung, N.T. (2016) *Int. J. Quantum Chem.*, DOI:10.1002/qua.25338.
56. Goodwin, E.J. and Legon, A.C. (1986) *J. Chem. Phys.*, **84** , 1988-1995.
57. Ruoff, R.S., Emilsson, T., Chuang, C., Klots, T.D. and Gutowsky, H.S. (1989) *J. Chem. Phys.*, **90** , 4069-4078.

58. Caminati, W., Melandri, S., Moreschini, P. and Favero, P.G. (1999) *Angew. Chem. Int. Edit. Engl.*, **38**, 2924-2925.
59. Van der Veken, B.J., Herrebout, W.A., Szostak, R., Shchepkin, D.N., Havlas, Z. and Hobza, P. (2001) *J. Am. Chem. Soc.*, **123**, 12290-12293.
60. MacKenzie, V.J. and Steer, R.P. (2001) *Can. J. Phys.*, **79**, 483-499.
61. Blanco, S., Lopez, J.C., Lesarri, A. and Alonso, J.L. (2002) *J. Mol. Structure*, **612**, 255-260.
62. Melikova, S.M., Rutkowski, K.S., Rodziewicz, P. and Koll, A. (2002) *Chem. Phys. Letters*, **352**, 301-310.
63. Van der Kerkhof, T., Bouwen, A., Goovaerts, E., Herrebout, W.A. and van der Veken, B.J. (2004) *Phys. Chem. Chem. Phys.*, **6**, 358-362.
64. Melikova, S.M., Rutkowski, K.S., Rodziewicz, P. and Koll, A. (2004) *J. Mol. Structure*, **705**, 49-61.
65. Rutkowski, K.S., Rodziewicz, P., Melikova, S.M., Herrebout, W.A., van der Veken, B.J. and Koll, A. (2005) *Chem. Phys.*, **313**, 225-243.
66. Delanoye, S.N., Herrebout, W.A. and van der Veken, B.J. (2005) *J. Phys. Chem. A*, **109**, 9836-9843.
67. Caminati, W., Lopez, J.C., Alonso, J.L. and Grabow, J.-U. (2005) *Angew. Chem.*, **117**, 3909-3912.
68. Serafin, M.M., Peebles, R.A. and Peebles, S.A. (2008) *J. Mol. Spectrosc.*, **250**, 1-7.
69. Favero, L.B., Giuliano, B.M., Maris, A., Melandri, S., Ottaviani, P., Velino, B. and Caminati, W. (2010) *Chem. Eur. J.*, **16**, 1761-1764.
70. Gopi, R., Ramanathan, N. and Sundararajan, K. (2017) *Spectrochim. Acta A*, **181**, 137-147.
71. Frisch, M.J., Trucks, G.W., Schlegel, H.B., Scuseria, G.E., Robb, M.A., Cheeseman, J.R., Scalmani, G., Barone, V., Petersson, G.A., Nakatsuji, H., Li, X., Caricato, M., Marenich, A.V., Bloino, J., Janesko, B.G., Gomperts, R., Mennucci, B., Hratchian, H. P., Ortiz, J.V., Izmaylov, A.F., Sonnenberg, J.L., Williams-Young, D., Ding, F., Lipparini, F., Egidi, F., Goings, J., Peng, B., Petrone, A., Henderson, T., Ranasinghe, D., Zakrzewski, V.G., Gao, J., Rega, N., Zheng, G., Liang, W., Hada, M., Ehara, M., Toyota, K., Fukuda, R., Hasegawa, J., Ishida, M., Nakajima, T., Honda, Y., Kitao, O., Nakai, H., Vreven, Y., Throssell, K., Montgomery, J.A., Jr., Peralta, J.E., Ogliaro, F., Bearpark, M.J., Heyd, J.J., Brothers, E.N., Kudin, K.N., Staroverov, V.N., Keith, T. A., Kobayashi, R., Normand, J., Raghavachari, K., Rendell, A.P., Burant, J.C., Iyengar, S.S., Tomasi, J., Cossi, M., Millam, J.M., Klene, M., Adamo, C., Cammi, R., Ochterski, J.W., Martin, R.L., Morokuma, K., Farkas, O., Foresman, J.B. and Fox, D.J. (2016) *Gaussian 16, Revision A.03*; Gaussian, Inc.: Wallingford, CT, USA.
72. Møller, C. and Plesset, M.S. (1934) *Phys. Rev.*, **46**, 618-622.
73. Dunning, T.H., Jr. (1989) *J. Chem. Phys.*, **90**, 1007-1023.
74. Kendall, R.A., Dunning, T.H., Jr. and Harrison, R.J. (1992) *J. Chem. Phys.*, **96**, 6796-6806.
75. Liu, B. and McLean, A.D. (1973) *J. Chem. Phys.*, **59**, 4557-4558.
76. Boys, S.F. and Bernardi, F. (1970) *Mol. Phys.*, **19**, 553-556.
77. Jeziorski, B., Moszynski, R. and Szalewicz, K. (1994) *Chem. Rev.*, **94**, 1887-1930.
78. Turney, J.M., Simmonett, A.C., Parrish, R.M., Hohenstein, E.G., Evangelista, F., Fermann, J.T., Mintz, B.J., Burns, L.A., Wilke, J.J., Abrams, M.L., Russ, N.J., Leininger, M.L., Janssen, C.L., Seidl, E.T., Allen, W.D., Schaefer III, H.F., King, R.A., Valeev, E.F., Sherrill, C.D. and Crawford, T.D. (2011) *WIREs Comput. Mol. Sci.*, DOI:10.1002/wcms.93.
79. Reed, A.E., Curtiss, L.A. and Weinhold, F. (1988) *Chem. Rev.*, **88**, 899-926.
80. Glendening, E.D., Badenhoop, J.K., Reed, A. E., Carpenter, J.E., Bohmann, J.A., Morales, C.M. and Weinhold, F. NBO (Version 3.1) Theoretical Chemistry Institute, University of Wisconsin, Madison, WI, U.S.A. <http://www.chem.wisc.edu/nbo5> (accessed 4 August 2010).
81. Hunter, E.P.L. and Lias, S.G. (1998) *J. Phys. Chem. Ref. Data*, **27**, 413-656.
82. Haynes, W.M. (Editor-in-Chief), *CRC Handbook of Chemistry and Physics*, 91st edition (2010-2011), CRC Press, Boca Raton, FL, U.S.A., pp. 10-189, 10-190.

Table 1. Structures and energies of the tetrel-bonded and hydrogen-bonded complexes of CH₃F with NH₃, H₂O, HF, PH₃, H₂S and HCl.

Electron donor	Tetrel-bonded complexes (this work)	Tetrel-bonded complexes (this work)	Tetrel-bonded complexes (t
	Structure	Point group	Energy/ H^a
NH ₃	staggered	C _{3v}	-196.0054976
H ₂ O	H ₂ O in plane	C _s	-215.8737344
HF	linear	C _{3v}	-239.8846826
PH ₃	eclipsed	C _{3v}	-482.2050298
H ₂ S	staggered	C _s	-538.4526257
HCl	staggered	C _s	-599.8584768

^a 1 $H = 2625.346583$ kJ mol⁻¹.

Table 2. Structures and energies of the tetrel-bonded and hydrogen-bonded complexes of CH₂F₂ with NH₃, H₂O, HF, PH₃, H₂S and HCl (structure 1).

Electron donor	Tetrel-bonded complexes (this work)	Tetrel-bonded complexes (this work)	Tetrel-bonded complexes (t
	Structure	Point group	Energy/ H^a
NH ₃	eclipsed	C _s	-295.1546672
H ₂ O	H ₂ O in plane	C _s	-315.0238975
HF	- ^b	C ₁	-339.0364084
PH ₃	staggered	C _s	-581.3531635
H ₂ S	H ₂ S almost in plane	C ₁	-637.6010776
HCl	staggered	C _s	-699.0061343

^a 1 $H = 2625.346583$ kJ mol⁻¹.

^b Structure relaxed to FH...F hydrogen-bonded isomer.

Table 3. Structures and energies of the tetrel-bonded and hydrogen-bonded complexes of CH₂F₂ with NH₃, H₂O, HF, PH₃, H₂S and HCl (structure 2).

Electron donor	Tetrel-bonded complexes (this work)	Tetrel-bonded complexes (this work)	Tetrel-bonded complexes (t
	Structure	Point group	Energy/ H^a
NH ₃	CH...N bonded	C _s	-295.1550717
H ₂ O	OH...F bonded	C ₁	-315.0237341
HF	FH...F bonded	C ₁	-339.0364084
PH ₃	PH...F bonded	C ₁	-581.3522423
H ₂ S	SH...F bonded	C ₁	-632.6019331
HCl	C...Cl bonded, staggered	C ₁	-699.0059246

^a 1 $H = 2625.346583$ kJ mol⁻¹.

Table 4. Structures and energies of the hydrogen-bonded and “reverse hydrogen-bonded” complexes of CHF₃ with NH₃, H₂O, HF, PH₃, H₂S and HCl.

Electron donor	“Reverse hydrogen-bonded” complexes (this work)	“Reverse hydrogen-bonded” complexes (this work)
	Structure	Point group
NH ₃	doubly NH...F bonded	C ₁
H ₂ O	CH...O bonded	C _s

Electron donor	“Reverse hydrogen-bonded” complexes (this work)	“Reverse hydrogen-bonded” complexes (this work)
HF	FH...F bonded	C _s
PH ₃	doubly PH...F bonded	C ₁
H ₂ S	doubly SH...F bonded	C _s
HCl	ClH...F bonded	C ₁

^a 1 $H = 2625.346583 \text{ kJ mol}^{-1}$.

Table 5. Interaction energies of the complexes of CH₃F, CH₂F₂ and CHF₃ with NH₃, H₂O, HF, PH₃, H₂S and HCl. Interaction energies of tetrel-bonded complexes are shown in bold type.

Electron donor	CH ₃ F complexes	CH ₃ F complexes	CH ₂ F ₂ complexes	CH ₂ F ₂ complexes	CH ₂ F ₂ complexes	CHF ₃ complexes	CHF ₃ complexes
	Tetrel-bonded (this work)	Hydrogen-bonded (ref. 26)	Tetrel-bonded structure 1 (this work)	Tetrel-bonded structure 2 (this work)	Hydrogen-bonded (ref. 26)	“Reverse hydrogen-bonded” (this work)	Hydrogen-bonded (ref. 27)
NH ₃	-5.35	-7.23	-8.83	-8.71 ^b	-9.52	-0.80 ^f	-13.65
H ₂ O	-4.99	-10.13	-9.53	-8.90 ^c	-9.91	-11.18 ^g	-11.25
HF	-3.44	-16.66	-9.82 ^a	-9.83 ^a	-10.60	-4.10 ^a	-6.40
PH ₃	-3.29	-4.10	-3.98	-1.90 ^d	-4.67	-1.35 ^d	-5.37
H ₂ S	-2.83	-6.28	-4.87	-5.52 ^e	-6.76	-1.70 ^e	-6.88
HCl	-2.24	-11.19	-2.47	-1.78	-7.25	-3.45 ^h	-6.08

^a Structure relaxed to FH...F-bonded isomer.^b Structure relaxed to CH...N-bonded isomer.

^c Structure relaxed to OH...F-bonded isomer.^d Structure relaxed to PH...F-bonded isomer.

^e Structure relaxed to SH...F-bonded isomer.^f Structure relaxed to NH...F-bonded isomer.

^g Structure relaxed to CH...O-bonded isomer.^h Structure relaxed to ClH...F-bonded isomer.

Table 6. SAPT energy decomposition analysis of the tetrel-bonded complexes of CH₃F and CH₂F₂ with NH₃, H₂O, HF, PH₃, H₂S and HCl.

CH₃F complexes

Partner molecule	Interaction energy/kJ mol ⁻¹	Interaction energy/kJ mol ⁻¹	Interaction energy/kJ mol ⁻¹	Interaction
	Exchange	Electrostatics	Induction	Dispersion
NH ₃	10.08	-10.99	-2.07	-5.93
H ₂ O	7.53	-8.57	-1.52	-5.32
HF	4.41	-5.14	-0.72	-3.84
PH ₃	8.38	-5.82	-1.23	-6.16
H ₂ S	8.21	-5.85	-1.16	-6.24
HCl	5.92	-3.63	-0.73	-5.48
CH ₂ F ₂ complexes	CH ₂ F ₂ com			
Partner molecule	Interaction energy/kJ mol ⁻¹	Interaction energy/kJ mol ⁻¹	Interaction energy/kJ mol ⁻¹	Interaction
	Exchange	Electrostatics	Induction	Dispersion
NH ₃	16.68	-19.26	-2.82	-8.43
H ₂ O	17.73	-20.37	-3.45	-8.99

HF	-	-	-	-
PH ₃	12.82	-9.58	-1.79	-8.61
H ₂ S	13.06	-11.26	-1.90	-8.19
HCl	8.13	-5.47	-1.08	-6.76

Table 7. SAPT energy decomposition analysis of the hydrogen-bonded complexes of CH₃F and CH₂F₂ with NH₃, H₂O, HF, PH₃, H₂S and HCl.

CH₃F complexes

Partner molecule	Interaction energy/kJ mol ⁻¹			
	Exchange	Electrostatics	Induction	Dispersion
NH ₃	17.73	-17.64	-3.58	-8.57
H ₂ O	23.37	-23.40	-6.16	-9.45
HF	38.82	-36.41	-15.89	-9.51
PH ₃	13.34	-9.42	-2.13	-8.94
H ₂ S	17.71	-14.41	-3.47	-9.22
HCl	31.22	-25.56	-9.38	-11.54
CH ₂ F ₂ complexes				
Partner molecule	Interaction energy/kJ mol ⁻¹			
	Exchange	Electrostatics	Induction	Dispersion
NH ₃	19.07	-20.01	-3.42	-10.29
H ₂ O	17.64	-20.32	-3.43	-8.97
HF	28.33	-25.37	-10.71	-8.11
PH ₃	13.25	-9.40	-1.88	-9.37
H ₂ S	17.24	-14.37	-2.43	-10.81
HCl	20.93	-16.68	-5.28	-9.72

Table 8. Major intermolecular interactions and second order perturbation energies of the tetrel-bonded and hydrogen-bonded complexes of CH₃F with NH₃, H₂O, HF, PH₃, H₂S and HCl. See Figure 1 and ref. 26 for numbering of atoms. Labels of interacting lone pair orbitals relate to the orientations of their axes and their s:p coefficient ratios..

Electron donor	Tetrel-bonded (this work)	Tetrel-bonded (this work)	Hydrogen-bonded (ref. 26)	Hydrogen-bonded (ref. 26)	Hydrogen-bonded (ref. 26)	Hydrogen-bonded (ref. 26)
	Partner molecule - CH ₃ F Interaction	Partner molecule - CH ₃ F Perturbation energy /kJ mol ⁻¹	Partner molecule - CH ₃ F Interaction	Partner molecule - CH ₃ F Perturbation energy /kJ mol ⁻¹	CH ₃ F - partner molecule Interaction	CH ₃ F - partner molecule Perturbation energy /kJ mol ⁻¹
NH ₃	lp(N) - σ*(CF)	4.85	lp(N) - σ*(CH3)	2.30	lp3(F) - σ*(NH7) lp1(F) - σ*(NH7)	4.52 0.33
H ₂ O	lp2(O) - σ*(CF)	3.51			lp3(F) - σ*(OH7) lp1(F) - σ*(OH7)	12.72 1.05

Electron donor	Tetrel-bonded (this work)	Tetrel-bonded (this work)	Hydrogen-bonded (ref. 26)	Hydrogen-bonded (ref. 26)	Hydrogen-bonded (ref. 26)	Hydrogen-bonded (ref. 26)
HF	lp1(F3) - $\sigma^*(CF1)$	1.97	$\sigma(F3H7)$ - $\sigma^*(CF4)$	1.09	lp3(F4) - $\sigma^*(F3H7)$ lp1(F4) - $\sigma^*(F3H7)$	44.22 4.27
PH ₃	lp(P) - $\sigma^*(CF)$	3.31	lp(P) - $\sigma^*(CH3)$	1.09	lp3(F) - $\sigma^*(PH8)$ lp1(F) - $\sigma^*(PH8)$	3.47 1.34
H ₂ S	lp2(S) - $\sigma^*(CF)$	3.85	lp2(S) - $\sigma^*(CH6)$	1.13	lp3(F) - $\sigma^*(SH7)$ lp1(F) - $\sigma^*(SH7)$	7.32 1.55
HCl	lp3(Cl) - $\sigma^*(CF)$	3.10			lp3(F) - $\sigma^*(ClH7)$ lp1(F) - $\sigma^*(ClH7)$	26.82 5.10

Table 9. Major intermolecular interactions and second order perturbation energies of the tetrel-bonded and hydrogen-bonded complexes of CH₂F₂ with NH₃, H₂O, HF, PH₃, H₂S and HCl (structure 1). See Figure 2 and ref. 26 for numbering of atoms. Labels of interacting lone pair orbitals relate to the orientations of their axes and their s:p coefficient ratios..

Electron donor	Tetrel-bonded (this work)	Tetrel-bonded (this work)	Tetrel-bonded (this work)	Tetrel-bonded (this work)	Hydrogen-bonded (ref. 26)	Hydrogen-bonded (ref. 26)	Hydrogen-bonded (ref. 26)	Hydrogen-bonded (ref. 26)
	Partner molecule - CH ₂ F ₂ Interaction	Partner molecule - CH ₂ F ₂ Perturbation energy /kJ mol ⁻¹	CH ₂ F ₂ - partner molecule Interaction	CH ₂ F ₂ - partner molecule Perturbation energy /kJ mol ⁻¹	Partner molecule - CH ₂ F ₂ Interaction	Partner molecule - CH ₂ F ₂ Perturbation energy /kJ mol ⁻¹	CH ₂ F ₂ - partner molecule Interaction	CH ₂ F ₂ - partner molecule Perturbation energy /kJ mol ⁻¹
NH ₃	lp(N) - $\sigma^*(CF1)$	2.34	lp3(F4) - $\sigma^*(NH7)$	0.92	lp(N) - $\sigma^*(CH3)$	2.76	σ (CH3) - $\sigma^*(NH7)$	1.00
H ₂ O	lp1(O) - $\sigma^*(CF1)$	1.55	lp3(F4) - $\sigma^*(OH7)$	2.30	lp1(O) - $\sigma^*(CF4)$	1.55	lp3(F3) - $\sigma^*(OH7)$	2.26
HF ^a			lp2(F4) - $\sigma^*(F3H7)$ lp3(F4) - $\sigma^*(F3H7)$ lp1(F4) - $\sigma^*(F3H7)$	18.66 7.45 2.97			lp2(F4) - $\sigma^*(F3H7)$ lp3(F4) - $\sigma^*(F3H7)$ lp1(F4) - $\sigma^*(F3H7)$	18.70 7.45 2.97

Electron donor	Tetrel-bonded (this work)	Tetrel-bonded (this work)	Tetrel-bonded (this work)	Tetrel-bonded (this work)	Hydrogen-bonded (ref. 26)	Hydrogen-bonded (ref. 26)	Hydrogen-bonded (ref. 26)	Hydrogen-bonded (ref. 26)
PH ₃	lp(P) - $\sigma^*(CF1)$	1.38	lp3(F4) - $\sigma^*(PH7)$ lp1(F4) - $\sigma^*(PH7)$	2.59 0.84	lp(P) - $\sigma^*(CH3)$	1.42	lp2(F4) - $\sigma^*(PH9)$	2.47
H ₂ S	lp2(S) - $\sigma^*(CF1)$	0.48	lp3(F4) - $\sigma^*(SH7)$	1.63	lp2(S) - $\sigma^*(CH3)$	1.38	lp2(F5) - $\sigma^*(SH8)$ lp2(F6) - $\sigma^*(SH7)$	1.09 1.0
HCl	lp3(Cl) - $\sigma^*(CF1)$	1.51	lp3(F4) - $\sigma^*(ClH7)$	1.05			lp2(F4) - $\sigma^*(ClH7)$ lp1(F4) - $\sigma^*(ClH7)$ lp3(F4) - $\sigma^*(ClH7)$	12.01 2.1 1.00

^a Tetrel-bonded structure relaxed to FH...F hydrogen-bonded isomer.

Table 10. Changes in the natural atomic charges, and total charge differences of the tetrel-bonded and hydrogen-bonded complexes of CH₃F with NH₃, H₂O, HF, PH₃, H₂S and HCl. See text for numbering of atoms. Mismatches between the total charge shifts between donor and acceptor molecules are due to rounding errors.

Electron donor	Tetrel-bonded (this work)	Tetrel-bonded (this work)	Tetrel-bonded (this work)	Tetrel-bonded (this work)	Hydrogen-bonded (ref. 26)	Hydrogen-bonded (ref. 26)	Hydrogen-bonded (ref. 26)	Hydrogen-bonded (ref. 26)
	CH ₃ F	CH ₃ F	Partner molecule	Partner molecule	CH ₃ F	CH ₃ F	Partner molecule	Partner molecule
	Atom	Change/ <i>me</i> _a	Atom	Change/ <i>me</i> _a	Atom	Change/ <i>me</i> _a	Atom	Change/ <i>me</i> _a
NH ₃	F C H4,H5,H6 Total	-12.3 6.8 1.2 -1.9	N N7,H8,H9 Total	-0.1 0.7 2.0	F C H3 H5,H6 Total	-12.9 -9.8 27.2 -1.5 1.5	N H7 H8,H9 Total	-12.5 16.1 -2.9 -1.6
H ₂ O	F C H4 H5,H6 Total	-10.9 5.2 -0.8 2.4 -1.7	O H7 H8 Total	-6.9 4.3 4.2 1.6	F C H3 H5,H6 Total	-16.6 -7.2 22.7 3.2 5.3	O H7 H8 Total	-26.1 21.1 -0.5 -5.4
HF	F1 C H4,H5,H6 Total	-7.2 1.8 1.0 -2.4	F3 H7 Total	-3.1 5.4 2.3	F4 C H2 H5,H6 Total	-17.9 -5.2 16.3 11.6 16.4	F3 H7 Total	-34.8 18.1 -16.5
PH ₃	F C H4,H5,H6 Total	-6.1 2.1 0.9 -1.3	P H7,H8,H9 Total	-13.0 4.8 1.4	F C H3 H5,H6 Total	-6.3 -2.4 11.4 0.0 2.7	P H8 H7,H9 Total	-6.7 -7.7 -2.8
H ₂ S	F C H4 H5,H6 Total	-5.8 1.8 0.4 0.9 -1.8	S H7,H8 Total	-4.3 3.1 1.9	F C H4 H5 H6 Total	-9.8 -3.9 2.1 2.7 12.1 3.2	S H7 H8 Total	-27.3 25.1 -1.5 -3.2

Electron donor	Tetrel-bonded (this work)	Tetrel-bonded (this work)	Tetrel-bonded (this work)	Tetrel-bonded (this work)	Hydrogen-bonded (ref. 26)	Hydrogen-bonded (ref. 26)	Hydrogen-bonded (ref. 26)	Hydrogen-bonded (ref. 26)
HCl	F C H4	-3.7 0.5 -0.1	Cl H7	-1.9 3.4	F C H2	-12.7 -3.4	Cl H7	-42.7 30
	H5,H6	0.9			H5,H6	12.0 8.1		
	Total	-1.5	Total	1.5	Total	12.1	Total	-12.2

^a 1 *me* = 1.602176 x 10⁻²² C.

Table 11. Changes in the natural atomic charges, and total charge differences of the tetrel-bonded and hydrogen-bonded complexes of CH₂F₂ with NH₃, H₂O, HF, PH₃, H₂S and HCl (structure 1). See text for numbering of atoms. Mismatches between the total charge shifts between donor and acceptor molecules are due to rounding errors.

Electron donor	Tetrel-bonded (this work)	Tetrel-bonded (this work)	Tetrel-bonded (this work)	Tetrel-bonded (this work)	Hydrogen-bonded (ref. 27)	Hydrogen-bonded (ref. 27)	Hydrogen-bonded (ref. 27)	Hydrogen-bonded (ref. 27)
	CH ₂ F ₂	CH ₂ F ₂	Partner molecule	Partner molecule	CH ₂ F ₂	CH ₂ F ₂	Partner molecule	Partner molecule
	Atom	Change/ <i>me</i> _a	Atom	Change/ <i>me</i> _a	Atom	Change/ <i>me</i> _a	Atom	Change/ <i>me</i> _a
NH ₃	F1 C F4	-5.9 1.8	N H7	-10.9 9.6	F5,F6 C	-8.5 -11.2	N H7	-11.5 0.
	H5,H6	-12.0 8.0	H8,H9	0.7	H3 H4	31.0 -3.4	H8,H9	6.0
	Total	-0.1	Total	0.1	Total	-0.6	Total	0.6
H ₂ O	F1 C F4	-1.9 -2.6	O H7 H8	-21.0 14.9	F3 C F4	-17.0 -2.7	O H7 H8	-20.9 14
	H5,H6	-17.0 11.2		5.2	H5,H6	-1.8 11.2		5.2
	Total	0.9	Total	-0.9	Total	0.9	Total	-0.9
HF ^b	F1 C F4	-0.0 -0.0	F3 H7	-0.0 0.1	F4 C F6	-23.5 -5.5	F3 H7	-25.4 15
	H5 H6	-0.1 0.0 0.0			H2 H5	12.0 17.4		
	Total	-0.1	Total	0.1	Total	10.4	Total	-10.4
PH ₃	F1 C F4	-1.0 -2.0	P H7	-18.9 1.4	F4 C F6	-3.7 -6.3	P H7 H8	-15.3 9.
	H5,H6	-4.6 4.9	H8,H9	7.7	H3 H5	-1.2 13.4	H9	5.3 -1.5
	Total	2.2	Total	-2.1	Total	0.1	Total	-2.2
H ₂ S	F1 C F4	-0.2 -1.4	S H7 H8	-16.6 14.1	F5,F6 C	-4.9 -7.6	S H7,H8	-20.1 9.
	H5 H6	-8.5 5.2 5.2		2.1	H3 H4	15.2 2.4		
	Total	0.3	Total	-0.4	Total	0.2	Total	-0.3
HCl	F1 C F4	-2.3 -1.7	Cl H7	1.1 -0.1	F4 C F6	-13.8 -5.7	Cl H7	-26.5 19
	H5,H6	-2.7 2.9			H2 H5	7.0 13.1 6.1		
	Total	-0.9	Total	1.0	Total	6.7	Total	-6.6

^a 1 *me* = 1.602176 x 10⁻²² C.

^b Tetrel-bonded structure relaxed to FH...F hydrogen-bonded isomer.

Figure Captions

Figure 1. Optimized structures of the tetrel-bonded complexes of CH_3F with NH_3 , H_2O , HF , PH_3 , H_2S and HCl .

Figure 2. Optimized structures of the tetrel-bonded complexes of CH_2F_2 with NH_3 , H_2O , HF , PH_3 , H_2S and HCl (structure 1).

Figure 3. Optimized structures of the tetrel-bonded complexes of CH_2F_2 with NH_3 , H_2O , HF , PH_3 , H_2S and HCl (structure 2).

Figure 4. Optimized structures of the “reverse hydrogen-bonded” complexes of CHF_3 with NH_3 , H_2O , HF , PH_3 , H_2S and HCl .

Figure 5. Plots of the interaction energies of the CH_3F complexes with NH_3 , H_2O , HF , PH_3 , H_2S and HCl *versus* (a) the gas phase basicities and (b) the polarizabilities of the partner molecules.

Figure 6. Plots of the interaction energies of the CH_2F_2 (structure 1) complexes with NH_3 , H_2O , HF , PH_3 , H_2S and HCl *versus* (a) the gas phase basicities and (b) the polarizabilities of the partner molecules.

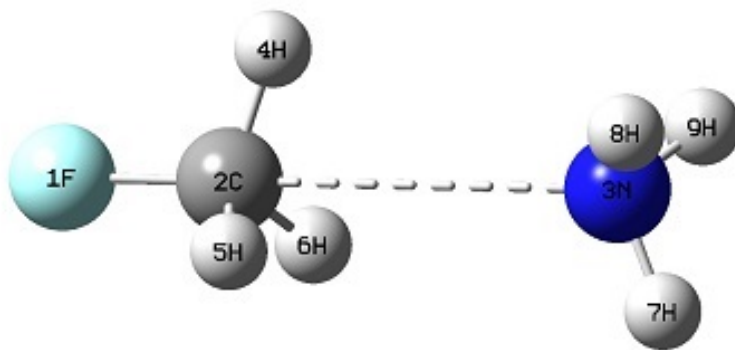
Figure 7. Plots of the intermolecular $\text{C}\dots\text{X}$ bond lengths of the tetrel-bonded complexes of CH_3F and CH_2F_2 with NH_3 , H_2O , HF , PH_3 , H_2S and HCl *versus* their interaction energies.

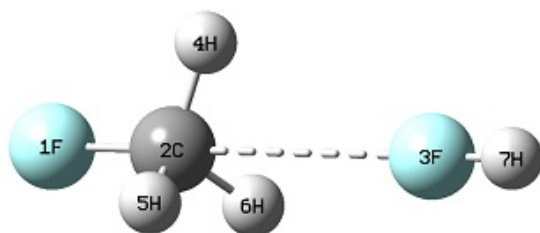
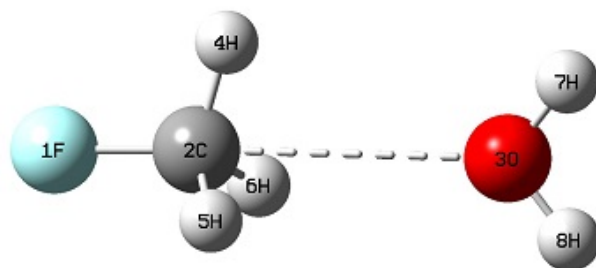
Figure 8. Plots of the changes of the intramolecular CF bond lengths of the tetrel-bonded complexes of CH_3F and CH_2F_2 with NH_3 , H_2O , HF , PH_3 , H_2S and HCl *versus* their interaction energies.

Figure 9. Plots of the mode wavenumber shifts of the CH_3F molecules of the tetrel-bonded complexes of CH_3F with NH_3 , H_2O , HF , PH_3 , H_2S and HCl *versus* their interaction energies: (a) CF stretching, (b) symmetric CH_3 bending.

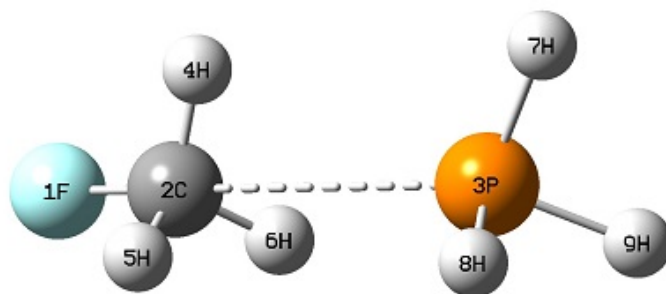
Figure 10. Plots of the mode wavenumber shifts of the CH_2F_2 molecules of the tetrel-bonded complexes of CH_2F_2 (structure 1) with NH_3 , H_2O , PH_3 , H_2S and HCl *versus* their interaction energies: (a) symmetric CH_2 stretching, (b) antisymmetric CH_2 stretching, (c) CH_2 bending.

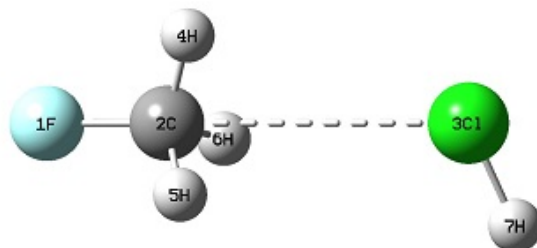
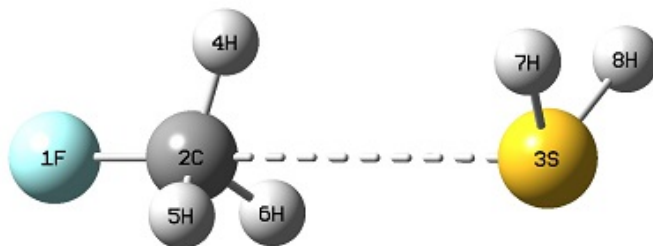
Figure 11. Plots of the atomic charge shifts of the F and C atoms of the complexes of CH_3F with NH_3 , H_2O , HF , PH_3 , H_2S and HCl : (a) tetrel-bonded, (b) hydrogen-bonded





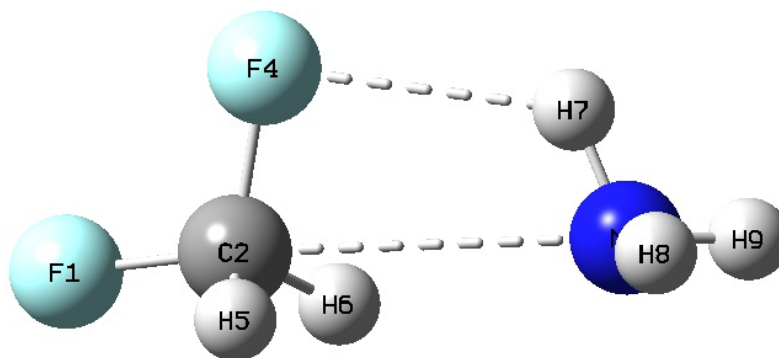
$\text{CH}_3\text{F} \cdot \text{NH}_3 \cdot \text{CH}_3\text{F} \cdot \text{H}_2\text{O}$ $\text{CH}_3\text{F} \cdot \text{HF}$

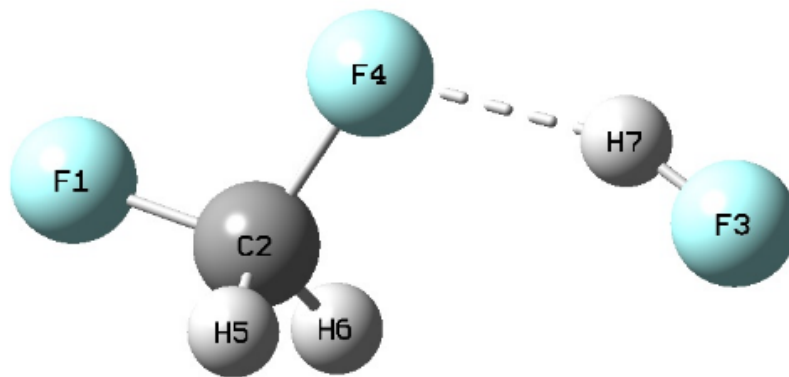
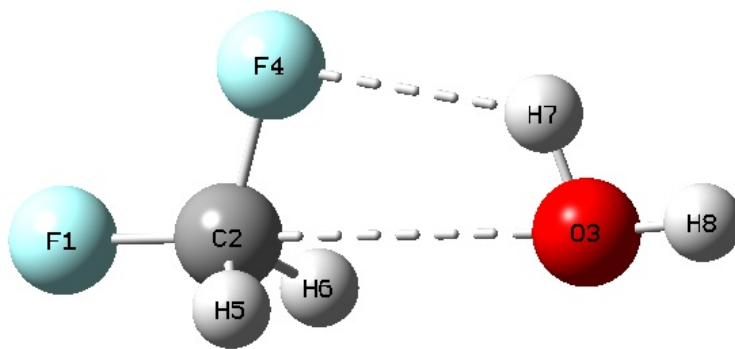




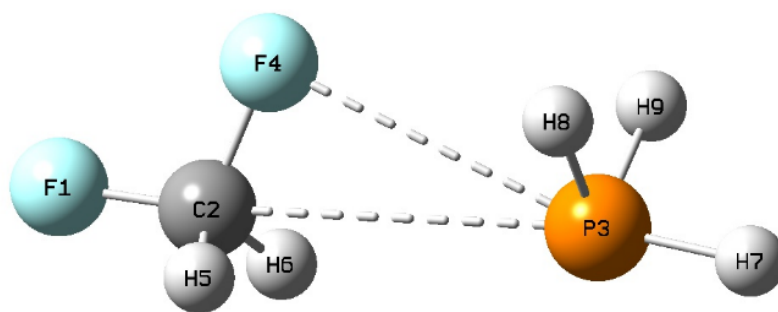
$\text{CH}_3\text{F} \cdot \text{PH}_3$ $\text{CH}_3\text{F} \cdot \text{H}_2\text{S}$ $\text{CH}_3\text{F} \cdot \text{HCl}$

Figure 1. Optimized structures of the tetrel-bonded complexes of CH_3F with NH_3 , H_2O , HF , PH_3 , H_2S and HCl .





$\text{CH}_2\text{F}_2 \cdot \text{NH}_3 \cdot \text{CH}_2\text{F}_2 \cdot \text{H}_2\text{O}$ $\text{CH}_2\text{F}_2 \cdot \text{HF}$



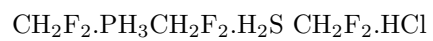
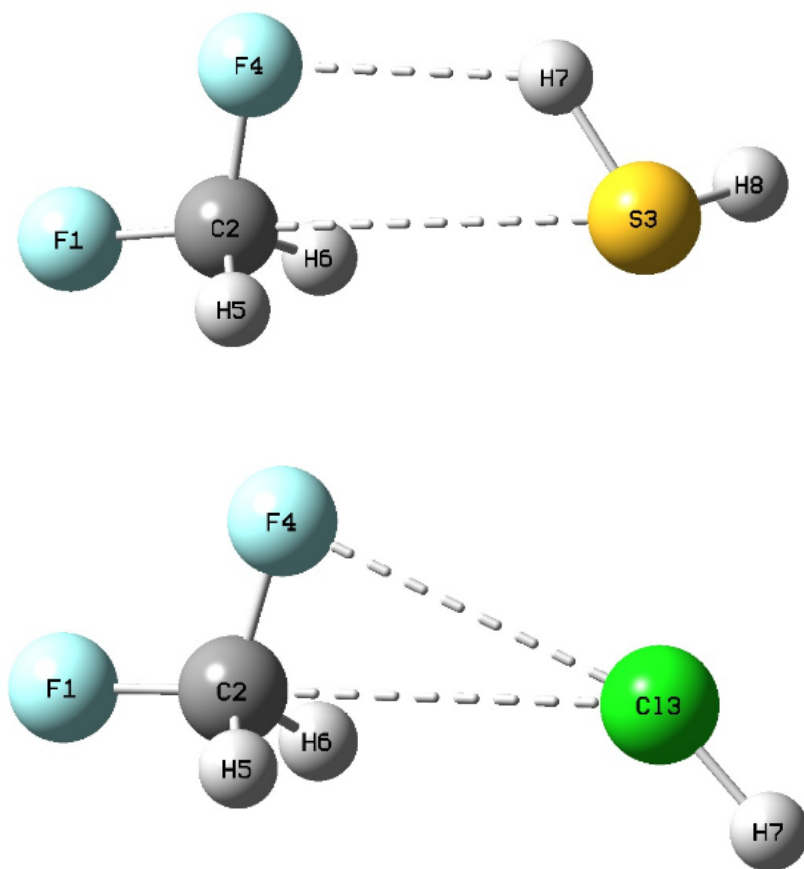
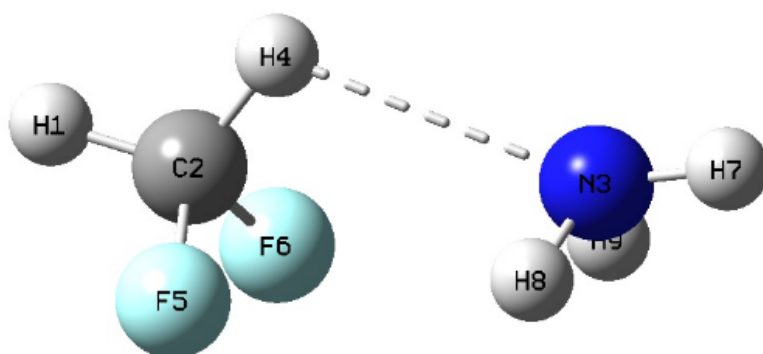
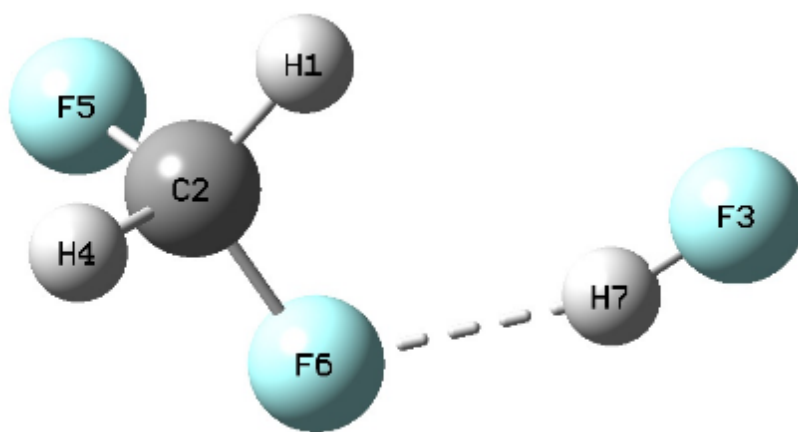
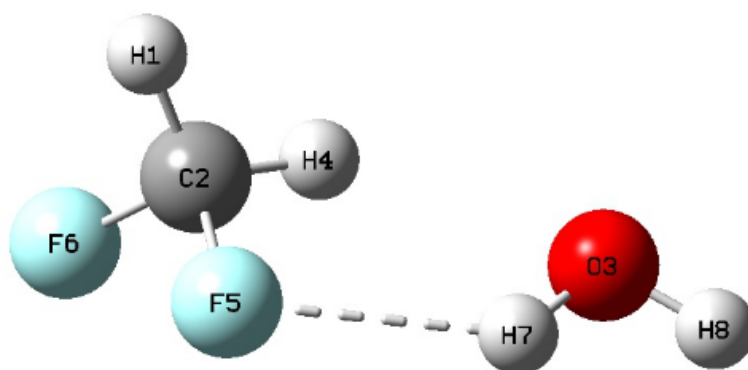
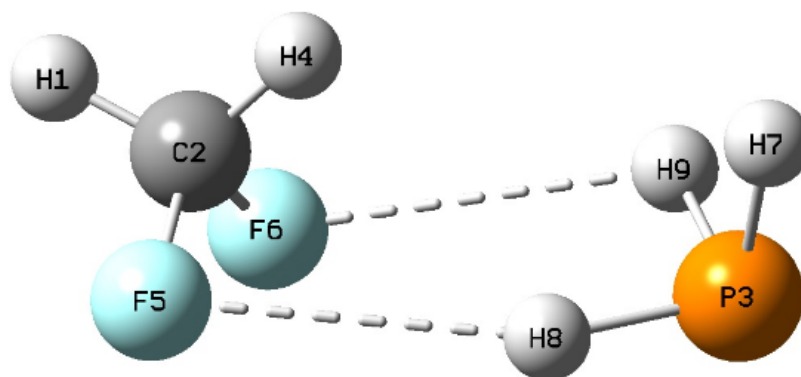


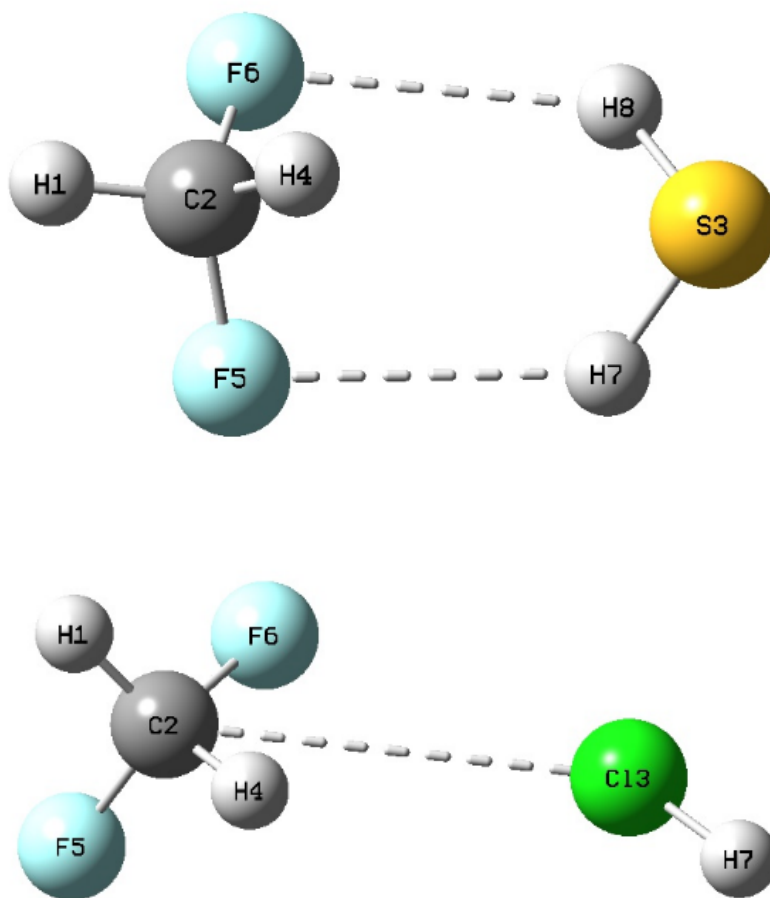
Figure 2. Optimized structures of the tetrel-bonded complexes of CH₂F₂ with NH₃, H₂O, HF, PH₃, H₂S and HCl (structure 1).





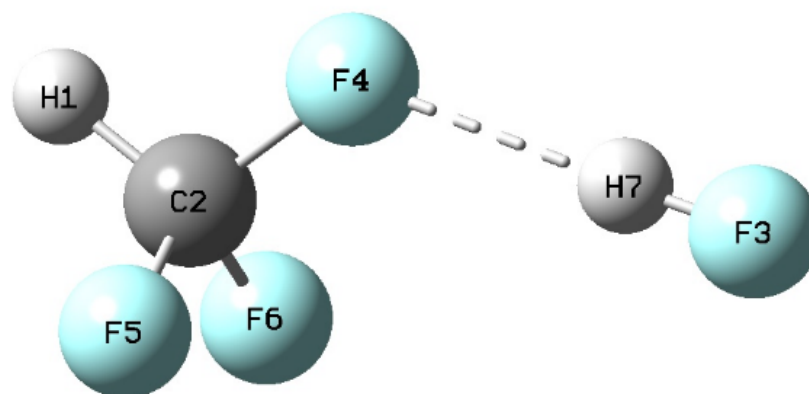
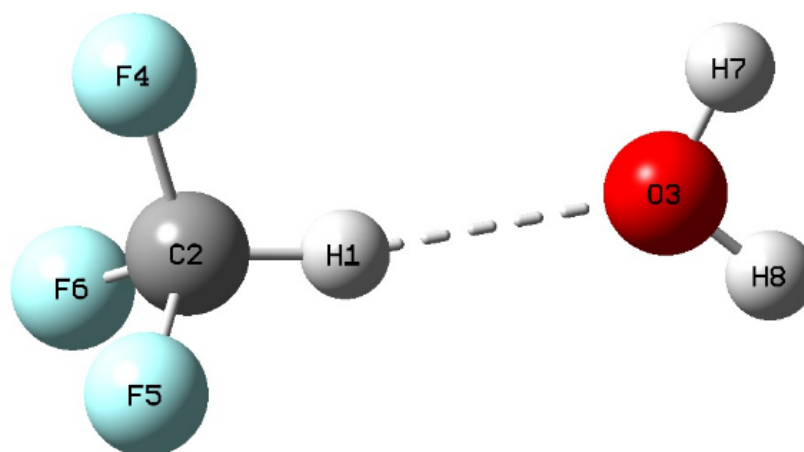
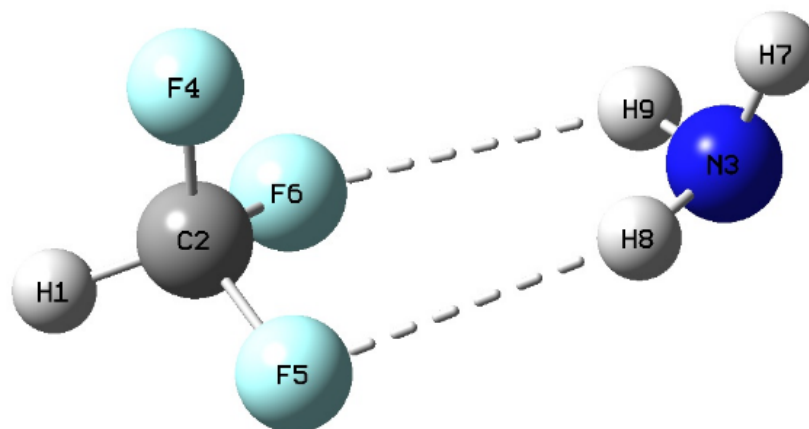
$\text{CH}_2\text{F}_2 \cdot \text{NH}_3\text{CH}_2\text{F}_2 \cdot \text{H}_2\text{O}$ $\text{CH}_2\text{F}_2 \cdot \text{HF}$



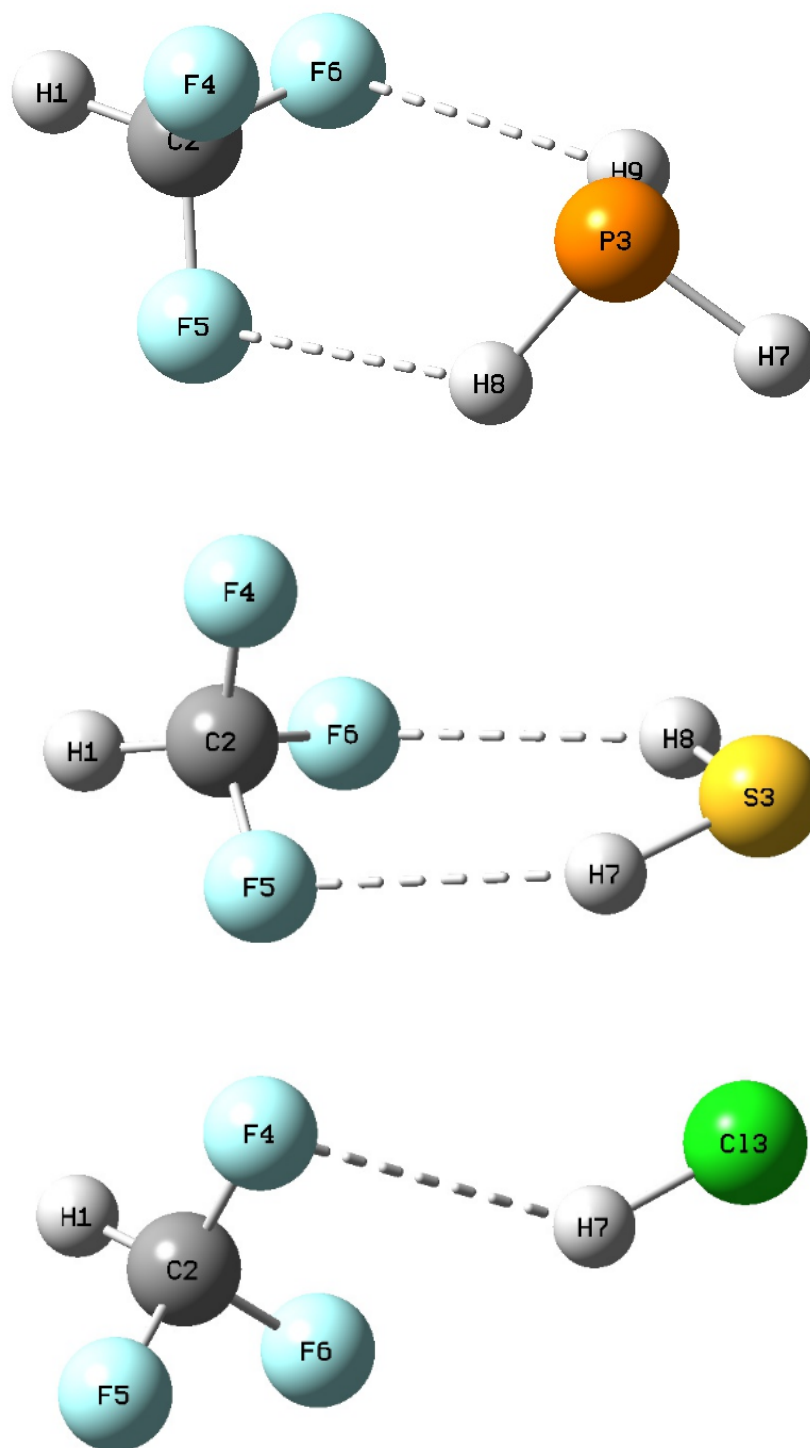


CH₂F₂.PH₃CH₂F₂.H₂S CH₂F₂.HCl

Figure 3. Optimized structures of the tetrel-bonded complexes of CH₂F₂ with NH₃, H₂O, HF, PH₃, H₂S and HCl (structure 2).

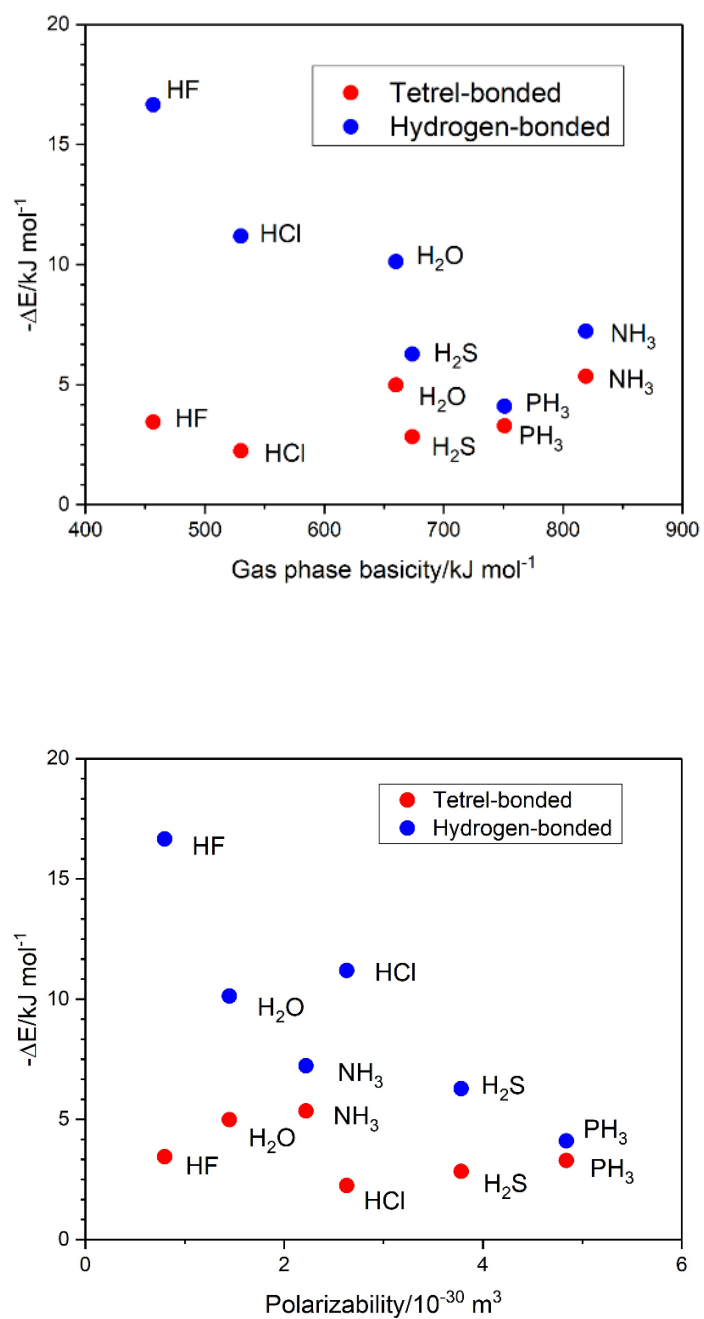


CHF₃.NH₃CHF₃.H₂O CHF₃.HF



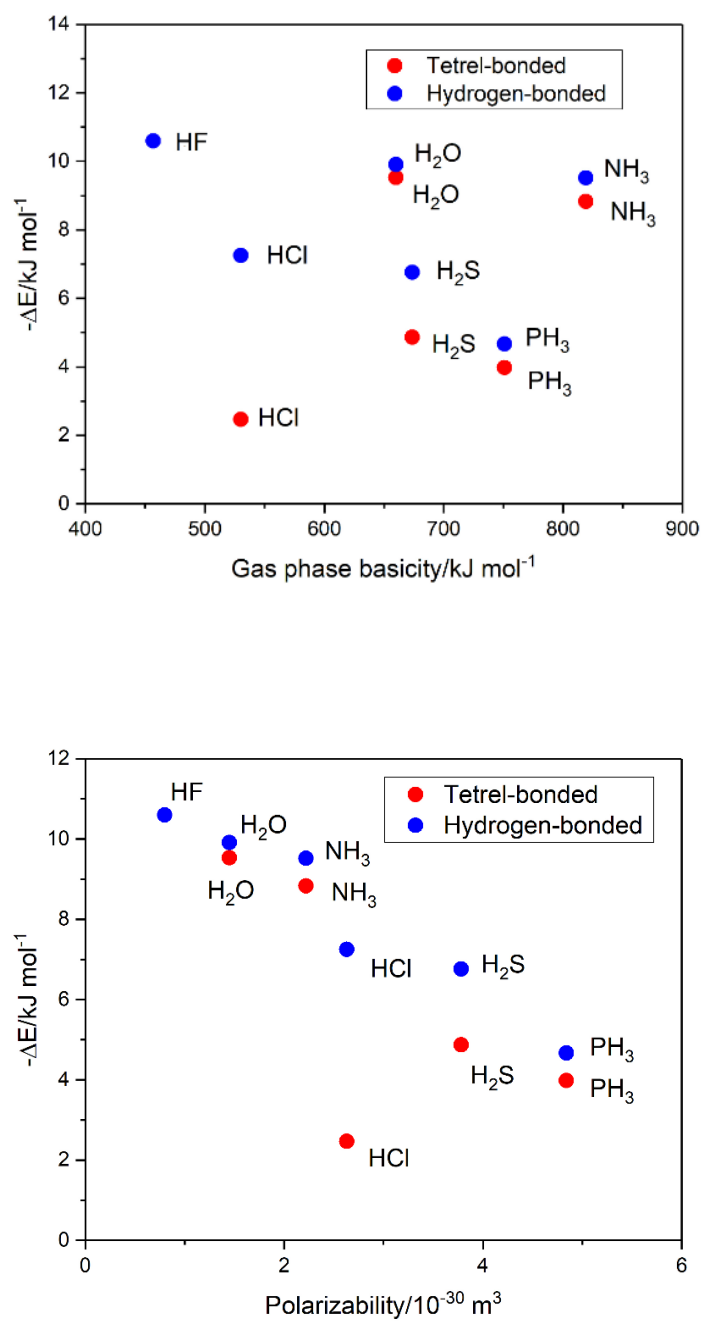
CHF₃.PH₃CHF₃.H₂S CHF₃.HCl

Figure 4. Optimized structures of the “reverse hydrogen-bonded” complexes of CHF₃ with NH₃, H₂O, HF, PH₃, H₂S and HCl.



(b)

Figure 5. Plots of the interaction energies of the CH_3F complexes with NH_3 , H_2O , HF , PH_3 , H_2S and HCl versus (a) the gas phase basicities and (b) the polarizabilities of the partner molecules.



(a) (b)

Figure 6. Plots of the interaction energies of the CH_2F_2 (structure 1) complexes with NH_3 , H_2O , HF , PH_3 , H_2S and HCl versus (a) the gas phase basicities and (b) the polarizabilities of the partner molecules.

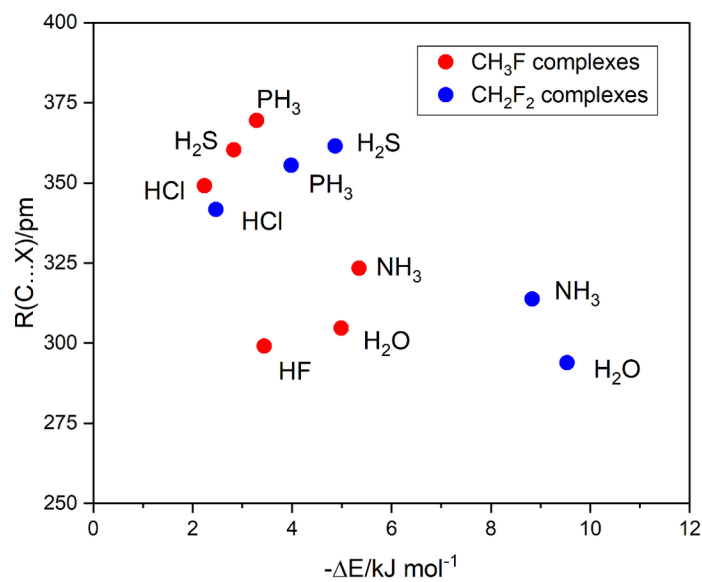


Figure 7. Plots of the intermolecular C...X bond lengths of the tetrel-bonded complexes of CH₃F and CH₂F₂ with NH₃, H₂O, HF, PH₃, H₂S and HCl *versus* their interaction energies.

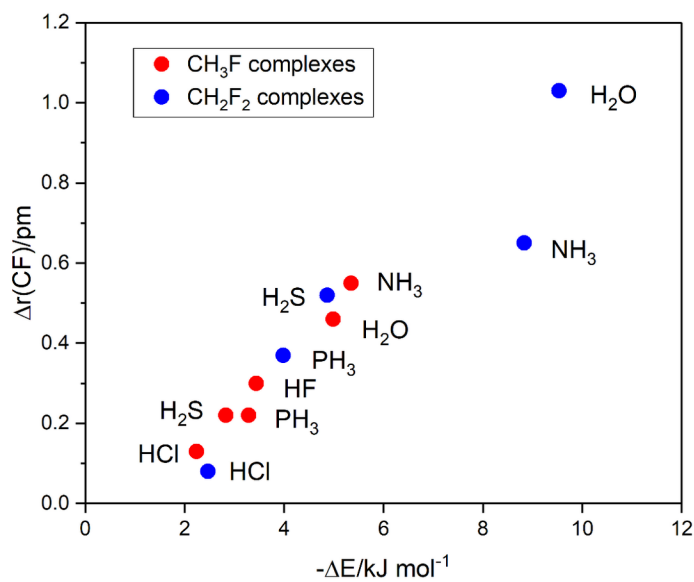
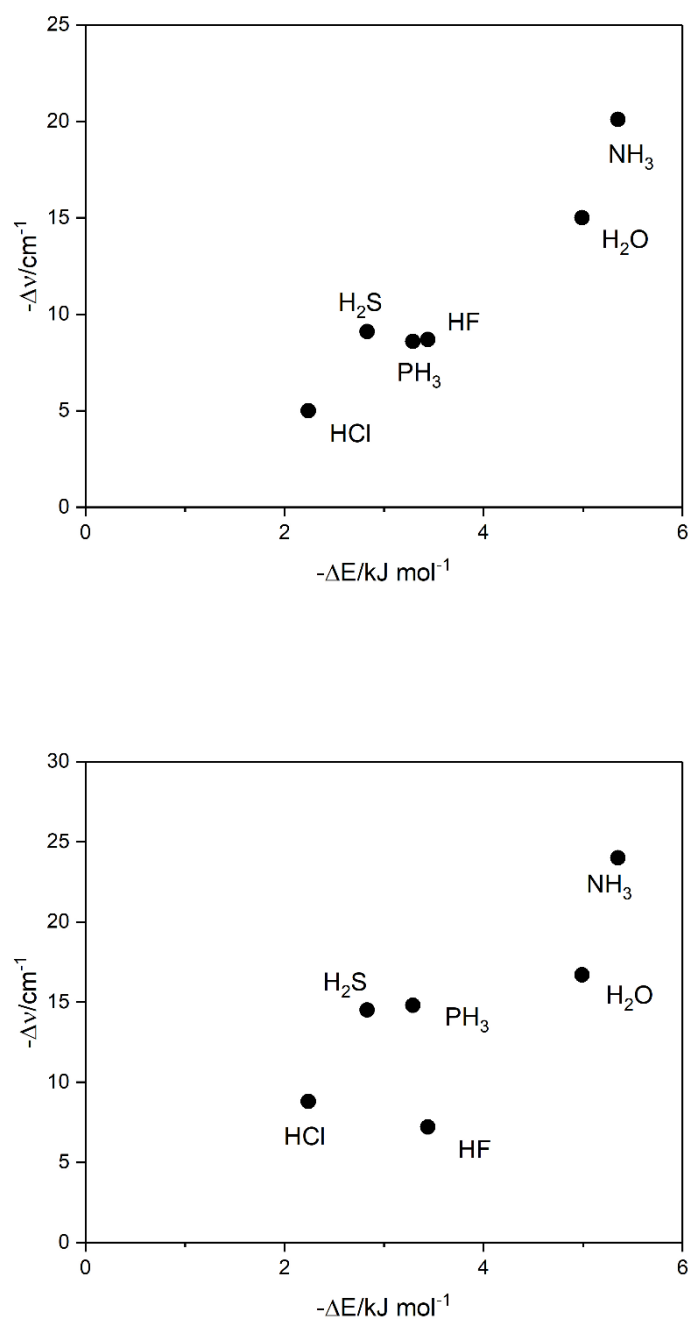
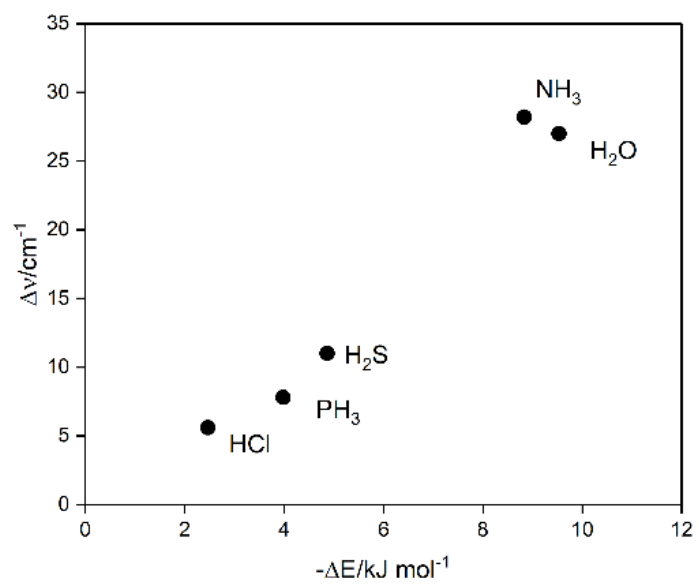
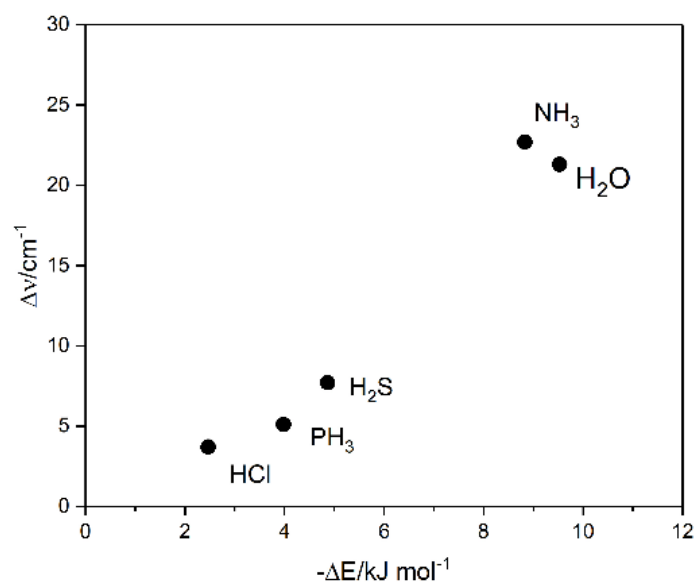


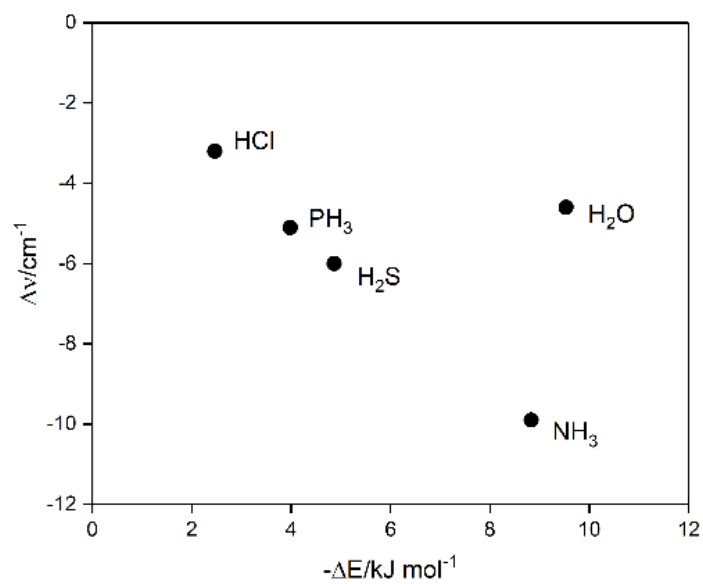
Figure 8. Plots of the changes of the intramolecular CF bond lengths of the tetrel-bonded complexes of CH₃F and CH₂F₂ with NH₃, H₂O, HF, PH₃, H₂S and HCl *versus* their interaction energies.



(b)

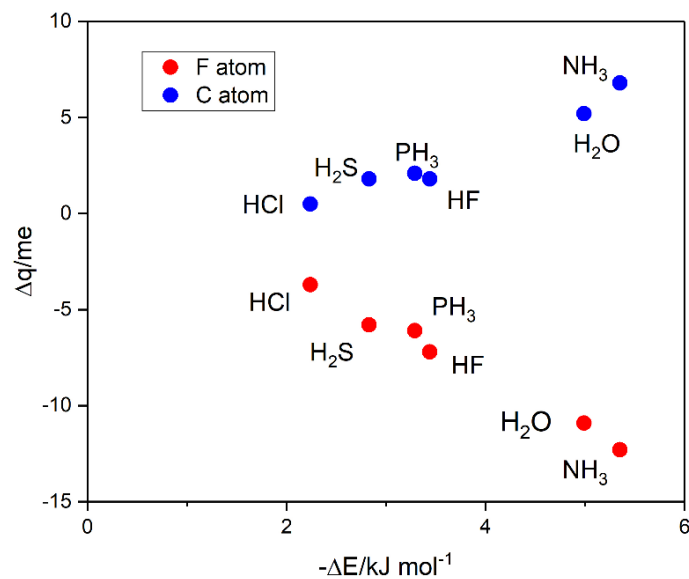
Figure 9. Plots of the mode wavenumber shifts of the CH₃F molecules of the tetrel-bonded complexes of CH₃F with NH₃, H₂O, HF, PH₃, H₂S and HCl *versus* their interaction energies: (a) CF stretching, (b) symmetric CH₃ bending.

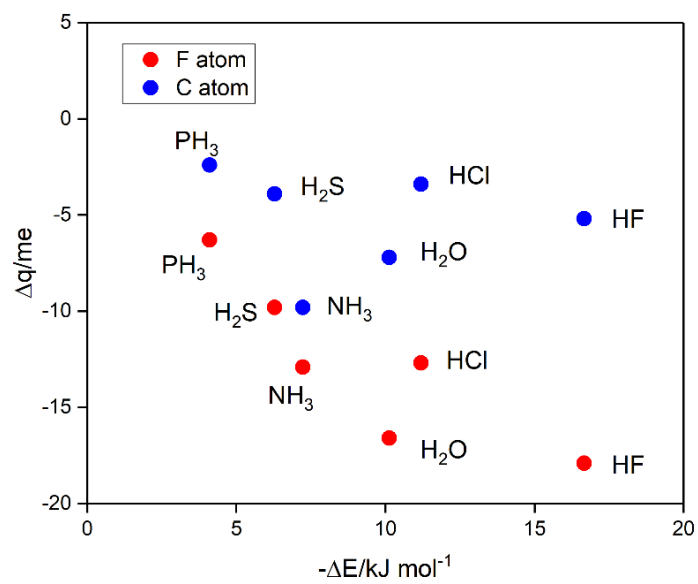




(a) (b) (c)

Figure 10. Plots of the mode wavenumber shifts of the CH₂F₂ molecules of the tetrel-bonded complexes of CH₂F₂ (structure 1) with NH₃, H₂O, PH₃, H₂S and HCl *versus* their interaction energies: (a) symmetric CH₂ stretching, (b) antisymmetric CH₂ stretching, (c) CH₂ bending.





(b)

Figure 11. Plots of the atomic charge shifts of the F and C atoms of the complexes of CH_3F with NH_3 , H_2O , HF , PH_3 , H_2S and HCl : (a) tetrel-bonded, (b) hydrogen-bonded